Supporting Information

Effect of Aromatic Ring Number and Substituent Arrangement on the Properties of Phenanthro[9,10-d]imidazole Derivatives for OLEDs

Agnieszka Krawiec [a], Jaijanarthanan Lingagouder [b], Agata Szlapa-Kula [a], Michał Filapek [a], Karol Erfurt[c], Przemyslaw Data [b,d*], Slawomir Kula [a*]

[a] *Institute of Chemistry, Faculty of Science and Technology, University of Silesia, Szkolna 9 St., 40-007 Katowice, Poland*

[b] *Department of Molecular Physics, Faculty of Chemistry, Lodz University of Technology, 90-543 Lodz, Poland*

[c] *Department of Organic Chemical Technology and Petrochemistry, Faculty of Chemistry, Silesian University of Technology, B. Krzywoustego 4, 44-100 Gliwice, Poland*

[d] *Department of Physics, Durham University, South Road, Durham DH1 3LE, United Kingdom*

1. Materials

Substrates and reactants: 9,10-Phenanthrenedione (≥99%, Sigma-Aldrich), ammonium acetate (puriss. p.a., ACS reagent, Ph. Eur., ≥98%, Sigma-Aldrich), benzaldehyde (>99.5%, Chemat), biphenyl-4-carboxaldehyde (99%, Sigma Aldrich), 2-napthaldehyde (95%, Sigma-Aldrich), 1-napthaldehyde (95%, Sigma-Aldrich), 9-anthracenecarboxaldehyde (97%, Sigma Aldrich), 9-phenanthrenecarboxaldehyde (97%, Sigma-Aldrich), 1-pyrenecarboxaldehyde (99%, Sigma-Aldrich), 3-perylenecarboxaldehyde (>95%, TCI). Anthracene-2-carbaldehyde and triphenylene-2-carboxaldehyde were obtained according to the procedures described in the literature [1-2].

Solvents: dichloromethane (pure, Chempur), methanol (MeOH, pure p.a., Chempur), acetonitrile (for HPLC-GC, ≥99.8% (GC), Sigma-Aldrich), dichloromethane (for HPLC, ≥99.8%, contains amylene as stabilizer, Sigma-Aldrich), chloroform (for HPLC, ≥99.8%, amylene stabilized, Sigma-Aldrich), methanol (MeOH, pure for analysis, Chempur), DMSO (pure for analysis, Chempur), tetrahydrofuran (pure for analysis, Eurochem BGD, glacial acetic acid (99,5% pure p. a, Chempur), dimethyl sulfoxide-d_6 (DMSO-d6, 99.8 atom % D, Sigma-Aldrich). All reactions were carried out under argon atmosphere.

2. General methods - measurements

Bruker NMR spectra were recorded using a Bruker Avance 500 instrument with DMSO-d6 as the solvent. Thermogravimetric analysis (TGA) was performed on a TA-TGA-55 device. UV/Vis spectra were measured using a Perkin Elmer UV-VIS Lambda Bio 40 spectrophotometer, while photoluminescence emission spectra were obtained with a Hitachi Fluorescence Spectrophotometer F-7100. Electrochemical measurements were conducted using an Eco Chemie Autolab PGSTAT128n potentiostat. A glassy carbon electrode (2 mm diameter) served as the working electrode, while a platinum coil and a silver wire were used as the auxiliary and reference electrodes, respectively. All potentials were referenced against ferrocene (Fc), which was employed as an internal standard. Cyclic and differential pulse voltammetry experiments were carried out in a standard one-compartment cell using dichloromethane (DCM) (Carlo Erba, HPLC grade) as the solvent, under an argon atmosphere. A 0.2 M solution of Bu_4NPF_6 (Aldrich, 99%) was used as the supporting electrolyte.

3. Synthesis

A mixture of aldehyde (6.00 mmol) (benzaldehyde (**0A**), biphenyl-4-carboxaldehyde (**0B**), 2-napthaldehyde (**0C**), 1-napthaldehyde (**0D**), 9-anthracenecarboxaldehyde (**0E**), 9-phenanthrenecarboxaldehyde (**0F**), anthracene-2-carbaldehyde (**0G**), triphenylene-2-carboxaldehyde (**0H**), 1-pyrenecarboxaldehyde (**0I**), 3-perylenecarboxaldehyde (**0J**)), 9,10-phenanthrenedione (1.25 g, 6.00 mmol), ammonium acetate (7.75 g, 100.00 mmol) and acetic acid (45 mL) was heated at reflux under argon atmosphere. After 24h, the solid was collected by filtration and washed with distilled water. Crude product was purified by double crystallization using methanol as solvent.

2-(phenyl)-1*H*-phenanthro[9,10-*d*]-imidazole (0A)

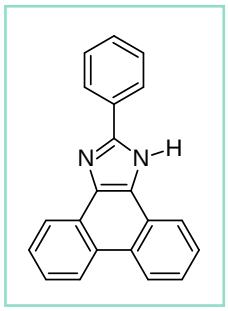

0A was obtained as brown solid with **63%** yield. **^{1}H NMR (500 MHz, DMSO) δ** 13.46 (s, 1H), 8.90 – 8.81 (m, 2H), 8.63 – 8.54 (m, 2H), 8.35 – 8.30 (m, 2H), 7.79 – 7.70 (m, 2H), 7.68 – 7.57 (m, 4H), 7.54 – 7.47 (m, 1H). **^{13}C NMR (125 MHz, DMSO) δ** 149.11, 136.99, 130.39, 129.25, 128.95, 127.70, 127.68, 127.54, 127.17, 127.08, 126.99, 126.15, 125.37, 125.16, 124.11, 123.75, 122.43, 122.00, 121.90. **HRMS (ESI)**: calcd. for $C_{21}H_{15}N_2$ $[M+H]^+$ 295.1235, found 295.1252.

2-(biphenyl-1-yl)-1*H*-phenanthro[9,10-*d*]-imidazole (0B)

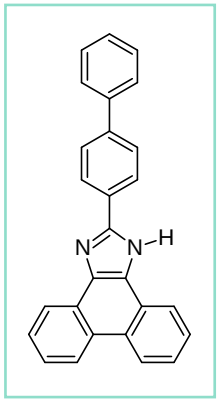

0B was obtained as brown solid with **83%** yield. **^{1}H NMR (500 MHz, DMSO) δ** 13.52 (s, 1H), 8.87 (dd, J = 17.5, 8.1 Hz, 2H), 8.62 (dd, J = 8.0, 1.4 Hz, 1H), 8.58 (dd, J = 8.0, 1.4 Hz, 1H), 8.42 (d, J = 8.5 Hz, 2H), 7.95 – 7.90 (m, 2H), 7.83 – 7.71 (m, 4H), 7.69 – 7.61 (m, 2H), 7.56 – 7.48 (m, 2H), 7.45 – 7.38 (m, 1H). **^{13}C NMR (125 MHz, DMSO) δ** 148.81, 140.65, 139.37, 137.12, 129.38, 129.04, 127.83, 127.78, 127.73, 127.57, 127.19, 127.14, 127.10, 126.97, 126.69, 126.67, 125.41, 125.20, 124.13, 123.77, 122.41, 122.03, 121.92. **HRMS (ESI)**: calcd. for $C_{27}H_{19}N_2$ $[M+H]^+$ 371.1548, found 371.1551.

2-(naphthalen-1-yl)-1*H*-phenanthro[9,10-*d*]-imidazole (0C)

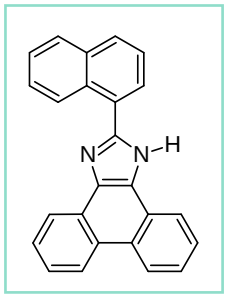

0C was obtained as brown solid with **65%** yield. **^{1}H NMR (500 MHz, DMSO) δ** 13.66 (s, 1H), 9.20 (d, J = 8.5 Hz, 1H), 8.94 – 8.86 (m, 2H), 8.67 (d, J = 7.9 Hz, 1H), 8.58 (d, J = 8.0 Hz, 1H), 8.18 – 8.11 (m, 2H), 8.09 (d, J = 8.1 Hz, 1H), 7.80 – 7.73 (m, 3H), 7.73 – 7.62 (m, 4H). **^{13}C NMR (125 MHz, DMSO) δ** 149.03, 137.00, 133.68, 130.63, 129.79, 128.42, 127.79, 127.79, 127.73, 127.51, 127.27, 127.24, 127.12, 127.09, 126.42, 126.36, 125.44, 125.31, 125.16, 124.12, 123.80, 122.43, 122.12, 121.93. **HRMS (ESI)**: calcd. for $C_{25}H_{17}N_2$ $[M+H]^+$ 345.1392, found 345.1416.

2-(naphthalen-2-yl)-1*H*-phenanthro[9,10-*d*]-imidazole (0D)

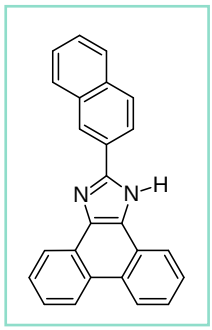

0D was obtained as brown solid with **60%** yield. **^{1}H NMR (500 MHz, DMSO) δ** 13.63 (s, 1H), 8.93 – 8.85 (m, 3H), 8.65 (dd, J = 7.9, 1.2 Hz, 1H), 8.61 (dd, J = 8.3, 1.0 Hz, 1H), 8.48 (dd, J = 8.6, 1.7 Hz, 1H), 8.17 – 8.08 (m, 2H), 8.02 (d, J = 7.7 Hz, 1H), 7.82 – 7.72 (m, 2H), 7.70 – 7.57 (m, 4H). **^{13}C NMR (125 MHz, DMSO) δ** 149.11, 137.17, 133.20, 132.98, 128.56, 128.34, 127.90, 127.86, 127.84, 127.79, 127.60, 127.23, 127.14, 126.99, 126.96, 126.86, 125.46, 125.23, 125.00, 124.16, 124.02, 123.79, 122.42, 122.04, 121.93. **HRMS (ESI)**: calcd. for $C_{25}H_{17}N_2$ $[M+H]^+$ 345.1392, found 345.1394.

2-(anthracen-9-yl)-1*H*-phenanthro[9,10-*d*]-imidazole (0E)

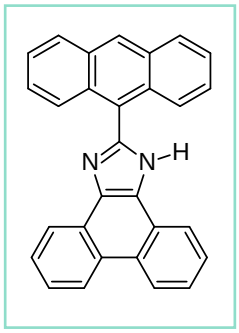

0E was obtained as brown solid with **41%** yield. **^{1}H NMR (500 MHz, DMSO) δ** 13.91 (s, 1H), 8.99 – 8.89 (m, 3H), 8.62 (dd, J = 8.0, 1.3 Hz, 1H), 8.40 (dd, J = 7.9, 1.3 Hz, 1H), 8.26 (d, J = 8.5 Hz, 2H), 7.81 (dd, J = 8.8, 1.0 Hz, 2H), 7.78 – 7.71 (m, 2H), 7.71 – 7.67 (m, 2H), 7.65 – 7.58 (m, 2H), 7.57 – 7.52 (m, 2H). **^{13}C NMR (125 MHz, DMSO) δ** 147.32, 137.37, 131.49, 131.22, 129.27, 129.01, 128.19, 128.02, 127.94, 127.71, 127.69, 127.66, 127.41, 126.50, 126.26, 126.20, 125.90, 125.62, 124.67, 124.32, 123.01, 122.49, 122.29. **HRMS (ESI)**: calcd. for $C_{29}H_{19}N_2$ $[M+H]^+$ 395.1548, found 395.1549.

2-(phenanthren-9-yl)-1*H*-phenanthro[9,10-*d*]-imidazole (0F)

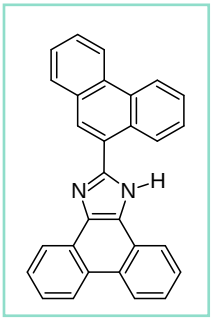

0F was obtained as brown solid with **81%** yield. **^{1}H NMR (500 MHz, DMSO) δ** 13.80 (s, 1H), 9.19 – 9.13 (m, 1H), 9.05 – 8.99 (m, 1H), 8.99 – 8.88 (m, 3H), 8.67 (dd, J = 8.1, 1.5 Hz, 1H), 8.59 (dd, J = 8.0, 1.4 Hz, 1H), 8.48 (s, 1H), 8.20 (dd, J = 7.8, 1.5 Hz, 1H), 7.86 – 7.74 (m, 6H), 7.73 – 7.65 (m, 2H). **^{13}C NMR (125 MHz, DMSO) δ** 149.37, 137.46, 131.05, 130.82, 130.61, 129.84, 129.56, 129.52, 128.48, 128.26, 128.03, 127.92, 127.80, 127.73, 127.65, 127.62, 127.60, 127.25, 125.95, 125.67, 124.63, 124.29, 123.79, 123.52, 122.93, 122.58, 122.44. **HRMS (ESI)**: calcd. for $C_{29}H_{19}N_2$ $[M+H]^+$ 395.1548, found 395.1563.

2-(anthracen-2-yl)-1*H*-phenanthro[9,10-*d*]-imidazole (0G)

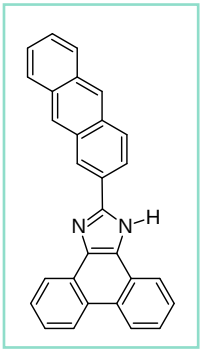

0G was obtained as brown solid with **95%** yield. **^{1}H NMR (500 MHz, DMSO) δ** 13.71 (s, 1H), 9.02 (s, 1H), 8.94 – 8.86 (m, 2H), 8.78 – 8.76 (m, 1H), 8.70 – 8.67 (m, 2H), 8.64 (dd, J = 8.0, 1.4 Hz, 1H), 8.49 (dd, J = 8.8, 1.7 Hz, 1H), 8.34 – 8.29 (m, 1H), 8.25 – 8.18 (m, 1H), 8.18 – 8.10 (m, 1H), 7.85 – 7.74 (m, 2H), 7.72 – 7.64 (m, 2H), 7.62 – 7.54 (m, 2H). **^{13}C NMR (125 MHz, DMSO) δ** 149.59, 137.74, 132.35, 132.26, 131.50, 131.43, 129.36, 128.70, 128.63, 128.49, 128.32, 128.10, 127.77, 127.73, 127.64, 127.45, 127.31, 126.73, 126.53, 126.45, 126.00, 125.75, 125.53, 124.65, 124.26, 122.87, 122.58, 122.43. **HRMS (ESI)**: calcd. for $C_{29}H_{19}N_2$ $[M+H]^+$ 395.1548, found 395.1557.

2-(triphenylen-2-yl)-1*H*-phenanthro[9,10-*d*]-imidazole (0H)

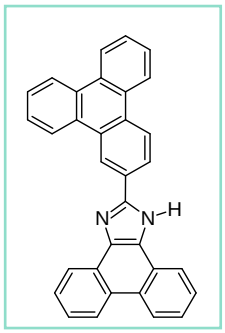

0H was obtained as brown solid with **77%** yield. **^{1}H NMR (500 MHz, DMSO) δ** 13.73 (s, 1H), 9.68 (s, 1H), 9.06 (dd, J = 8.3, 2.8 Hz, 2H), 8.96 – 8.86 (m, 5H), 8.74 – 8.67 (m, 2H), 8.63 (d, J = 7.4 Hz, 1H), 7.93 – 7.87 (m, 1H), 7.87 – 7.74 (m, 5H), 7.74 – 7.65 (m, 2H). **^{13}C NMR (125 MHz, DMSO) δ** 149.03, 137.00, 133.68, 130.63, 129.79, 128.42, 127.79, 127.79, 127.73, 127.51, 127.27, 127.24, 127.12, 127.09, 126.42, 126.36, 125.44, 125.31, 125.16, 124.12, 123.80, 122.43, 122.12, 121.93. **HRMS (ESI)**: calcd. for $C_{33}H_{21}N_2$ $[M+H]^+$ 445.1705, found 445.1713.

2-(pyren-1-yl)-1*H*-phenanthro[9,10-*d*]-imidazole (0I)

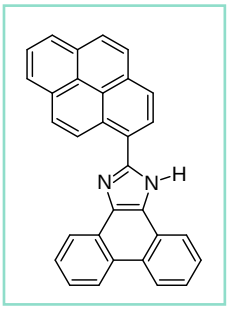

0I was obtained as brown solid with **91%** yield. **^{1}H NMR (500 MHz, DMSO) δ** 13.83 (s, 1H), 9.62 (d, J = 9.3 Hz, 1H), 8.96 – 8.88 (m, 2H), 8.76 (dd, J = 7.9, 1.4 Hz, 1H), 8.71 (d, J = 8.0 Hz, 1H), 8.66 (dd, J = 8.0, 1.4 Hz, 1H), 8.54 (d, J = 8.0 Hz, 1H), 8.42 – 8.36 (m, 3H), 8.31 (s, 2H), 8.16 (t, J = 7.6 Hz, 1H), 7.83 – 7.76 (m, 2H), 7.73 – 7.66 (m, 2H). **^{13}C NMR (125 MHz, DMSO) δ** 149.92, 137.84, 131.86, 131.45, 130.88, 129.04, 128.94, 128.82, 128.29, 128.18, 128.09, 127.90, 127.85, 127.78, 127.64, 127.59, 127.16, 126.33, 126.23, 126.00, 125.74, 125.35, 125.30, 124.91, 124.64, 124.32, 124.28, 122.93, 122.72, 122.52. **HRMS (ESI)**: calcd. for $C_{31}H_{19}N_2$ $[M+H]^+$ 419.1548, found 419.1554.

2-(perylen-3-yl)-1*H*-phenanthro[9,10-*d*]-imidazole (0J)

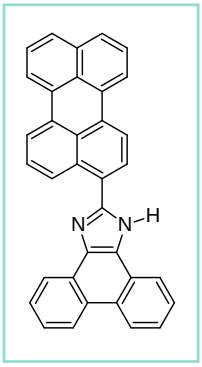

0J was obtained as brown solid with **23%** yield. **^{1}H NMR (500 MHz, DMSO) δ** 13.70 (s, 1H), 9.23 (dd, J = 8.5, 0.9 Hz, 1H), 8.91 (dd, J = 16.6, 8.3 Hz, 2H), 8.68 (dd, J = 8.0, 1.4 Hz, 1H), 8.64 – 8.58 (m, 2H), 8.54 (ddd, J = 7.9, 3.8, 1.1 Hz, 2H), 8.48 (d, 1H), 8.19 (d, J = 7.9 Hz, 1H), 7.88 (dd, J = 11.0, 8.1 Hz, 2H), 7.81 – 7.72 (m, 3H), 7.72 – 7.66 (m, 2H), 7.62 (dt, J = 8.7, 7.7 Hz, 2H). **^{13}C NMR (125 MHz, DMSO) δ** 149.36, 137.60, 134.71, 132.49, 132.22, 131.16, 131.02, 130.58, 129.07, 129.02, 128.61, 128.27, 128.22, 128.17, 128.04, 127.82, 127.74, 127.60, 127.51, 127.22, 126.00, 125.72, 124.62, 124.29, 122.84, 122.68, 122.46, 122.03, 121.76, 121.71, 120.75. **HRMS (ESI)**: calcd. for $C_{35}H_{21}N_2$ $[M+H]^+$ 469.1705, found 469.1707.

4. ^{1}H NMR, ^{13}C NMR and HRMS spectra

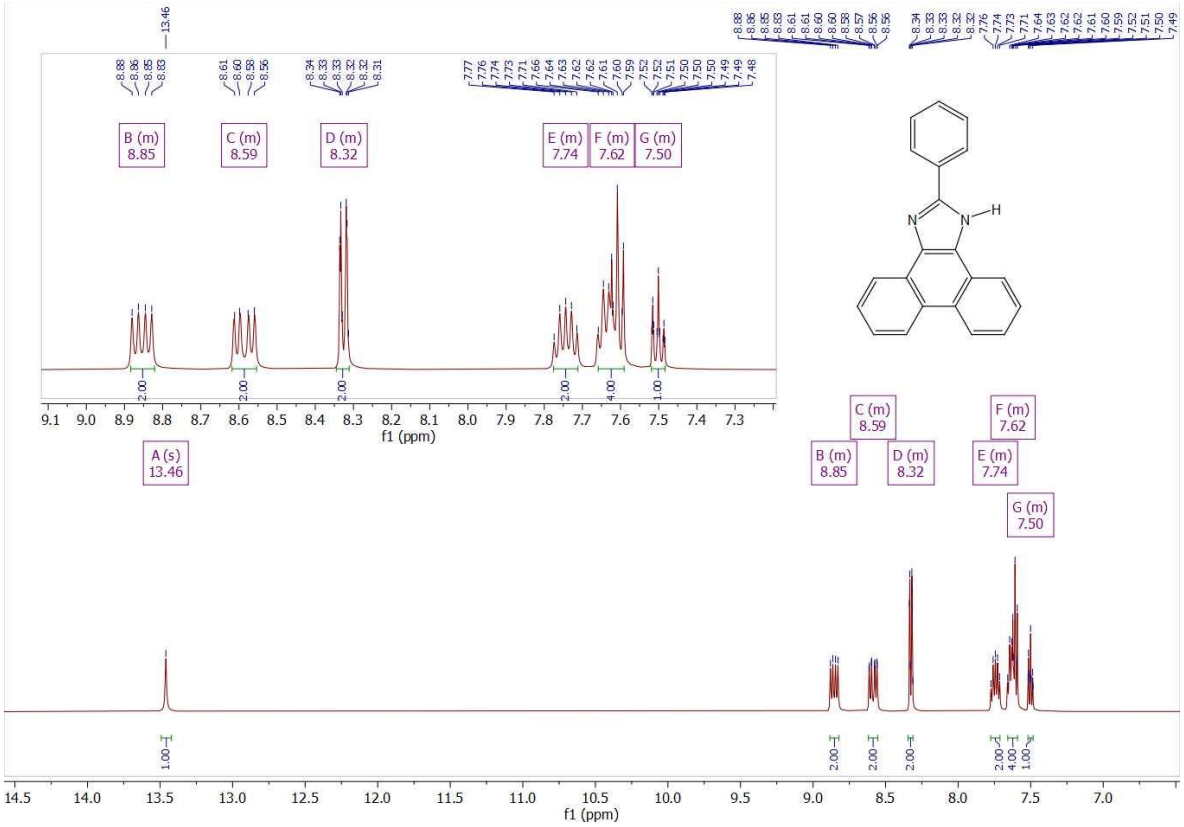

^{1}H NMR of 0A

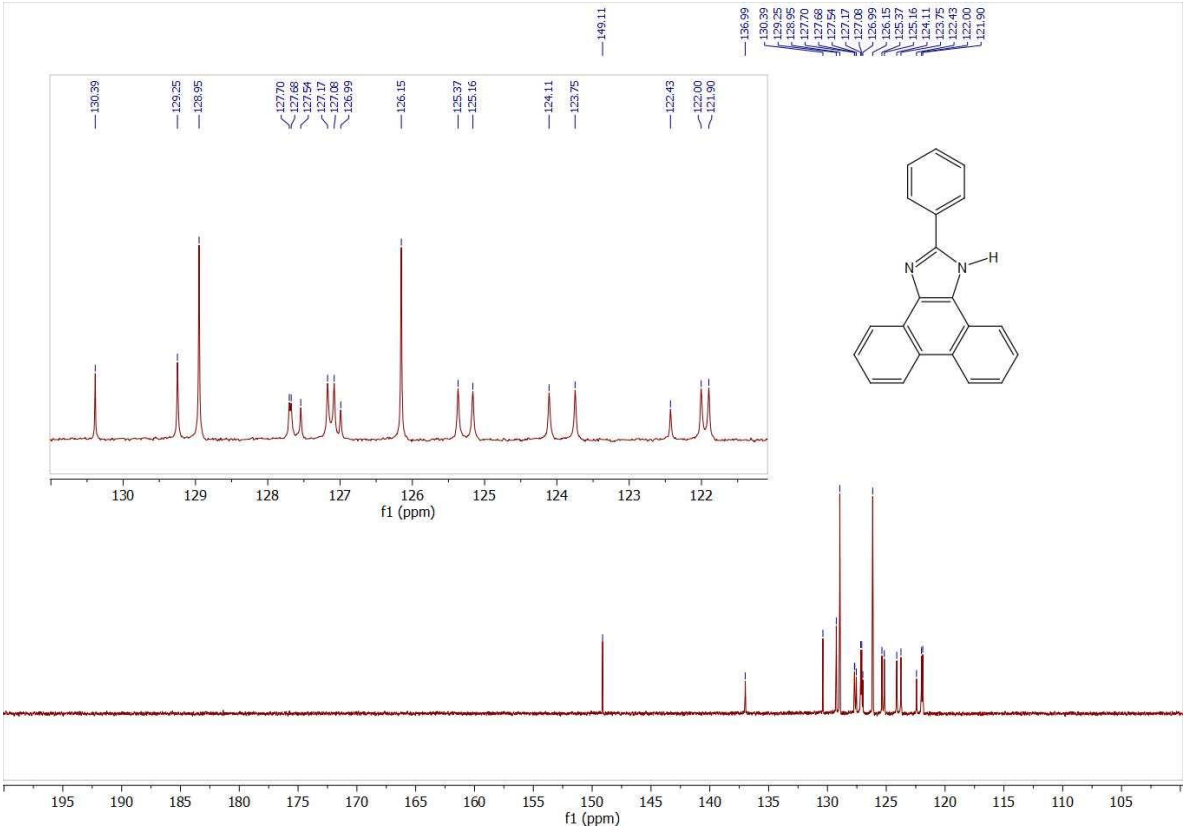

^{13}C NMR of 0A

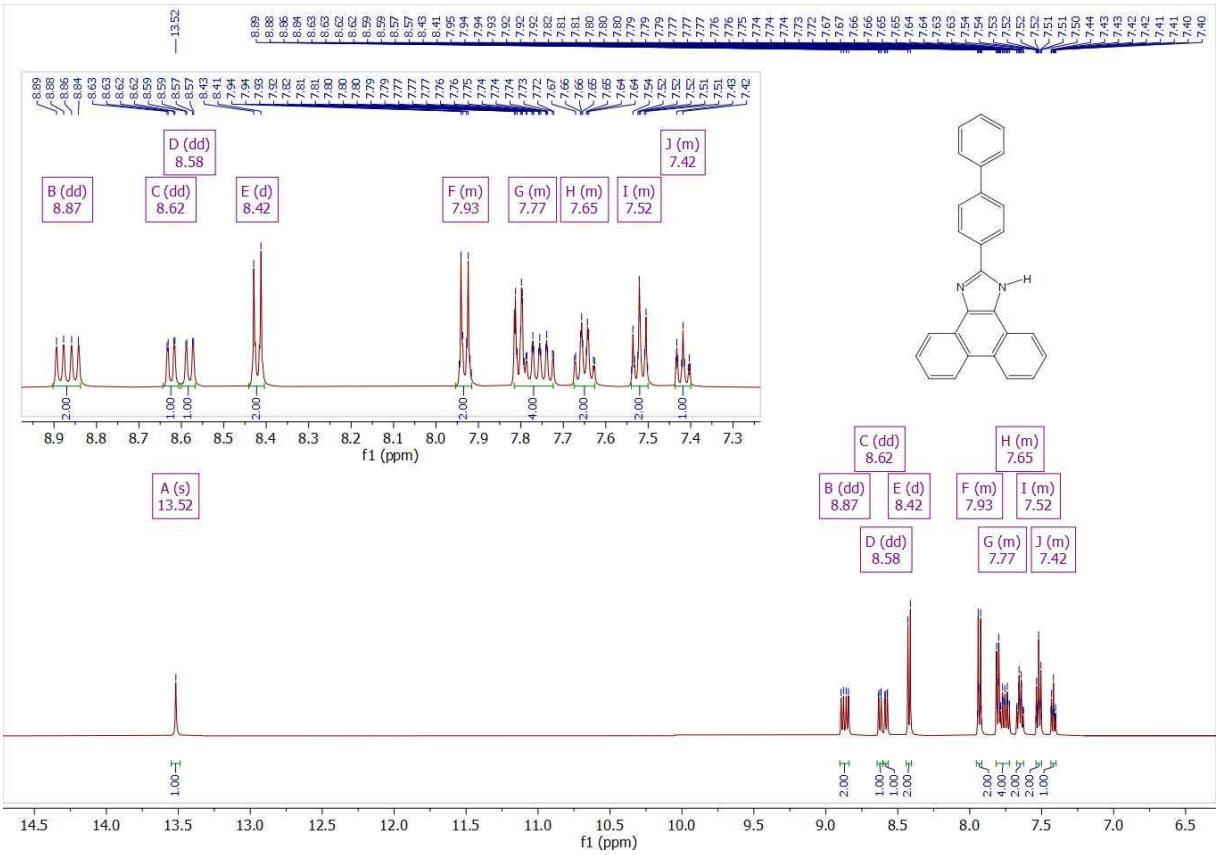

^{1}H NMR of 0B

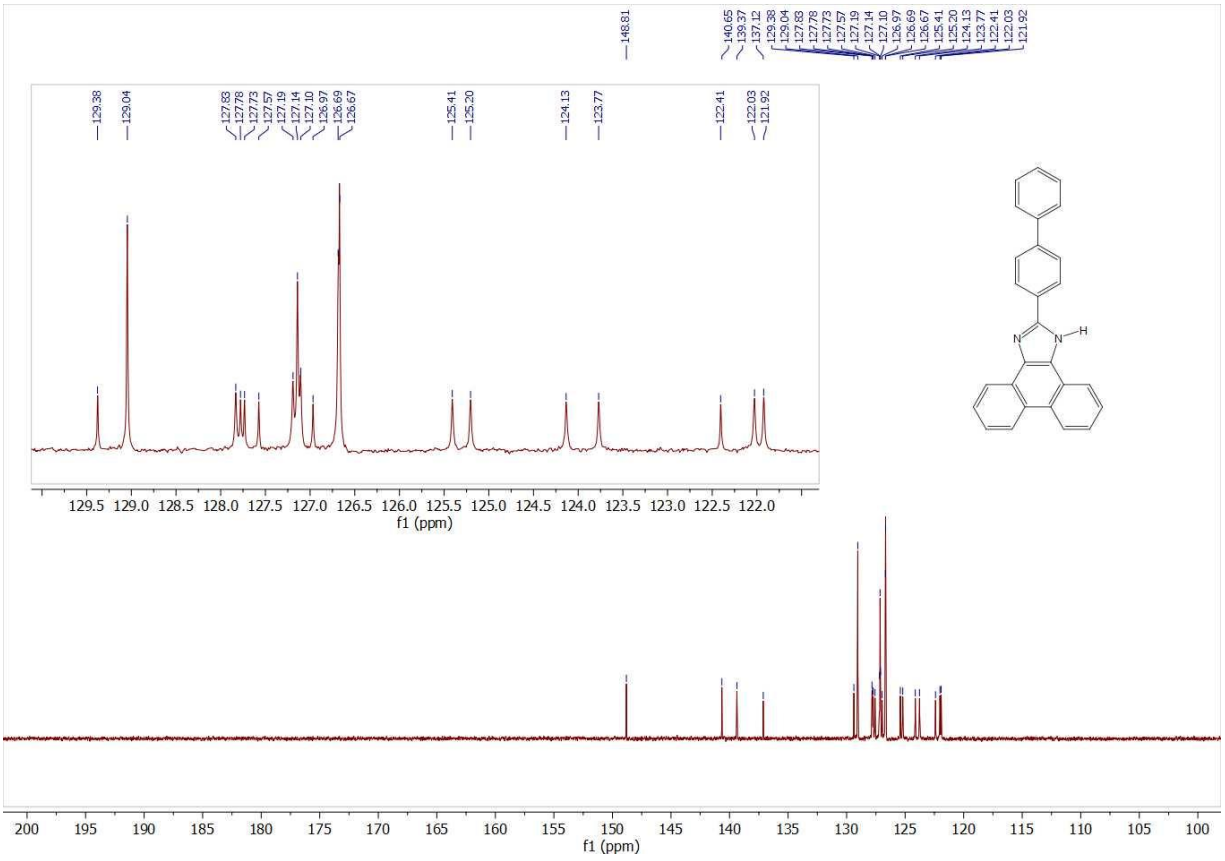

^{13}C NMR of 0B

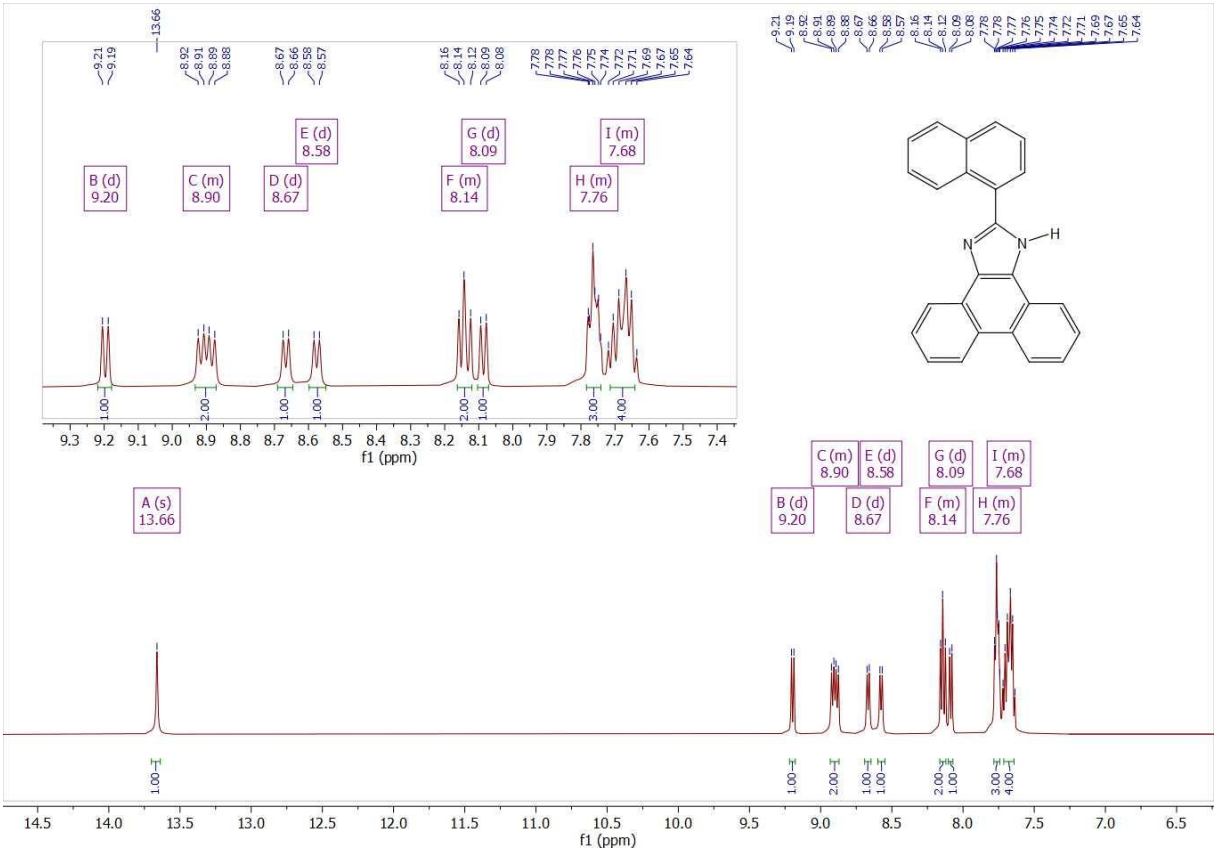

^{1}H NMR of 0C

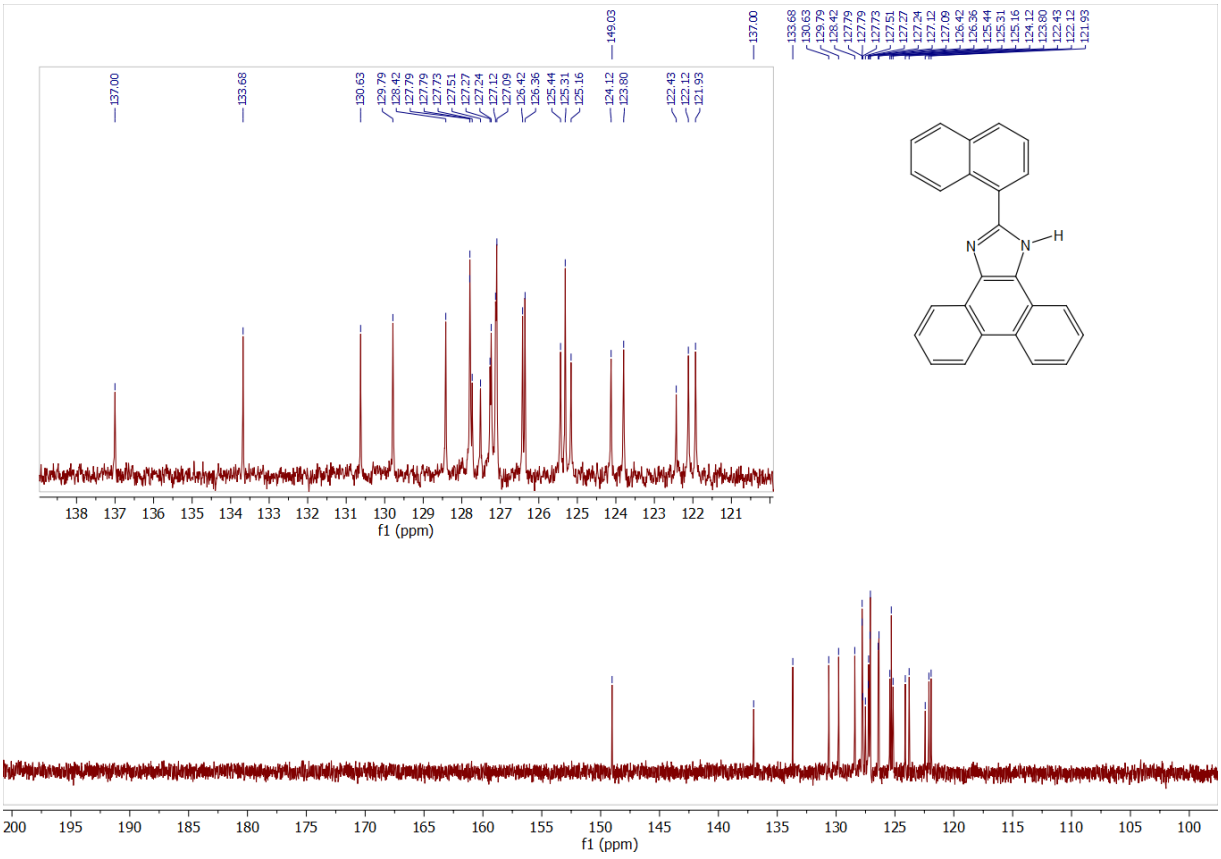

^{13}C NMR of 0C

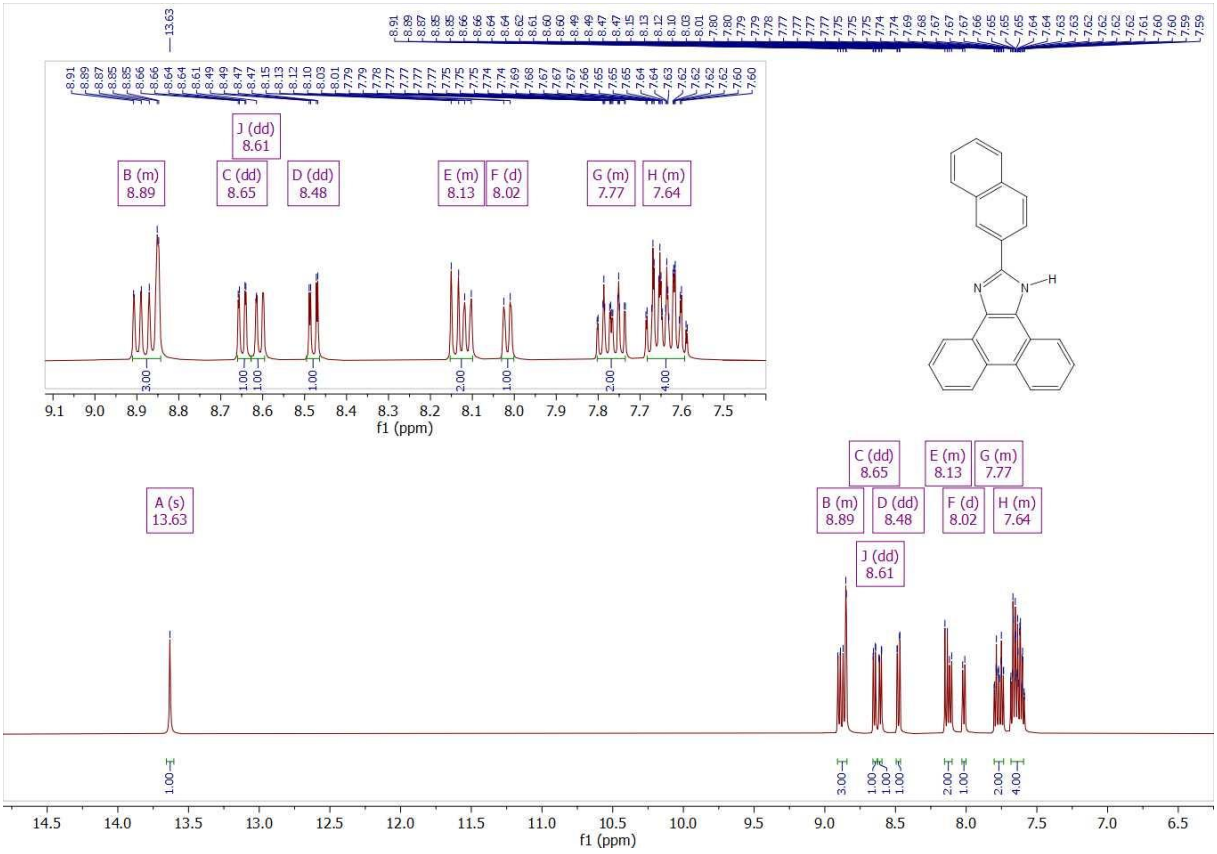

^{1}H NMR of 0D

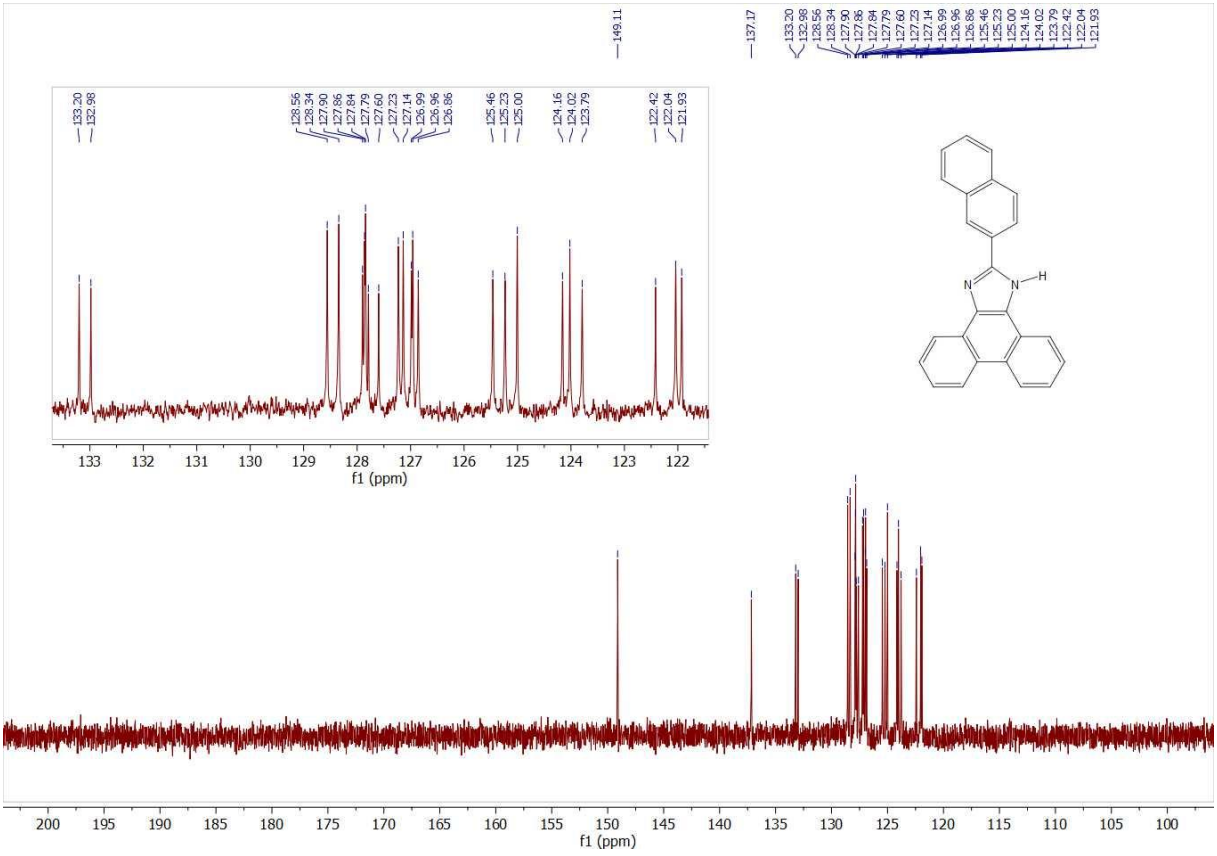

^{13}C NMR of 0D

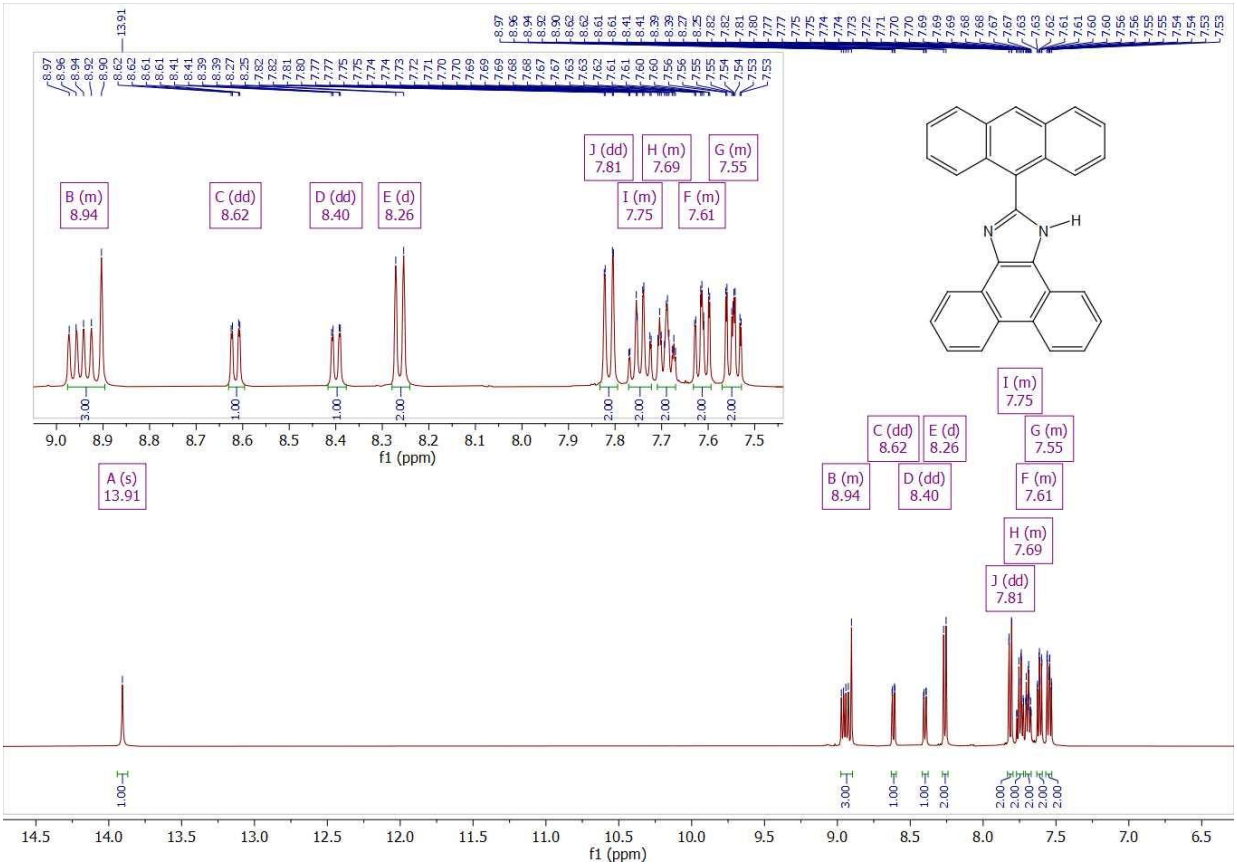

^{1}H NMR of 0E

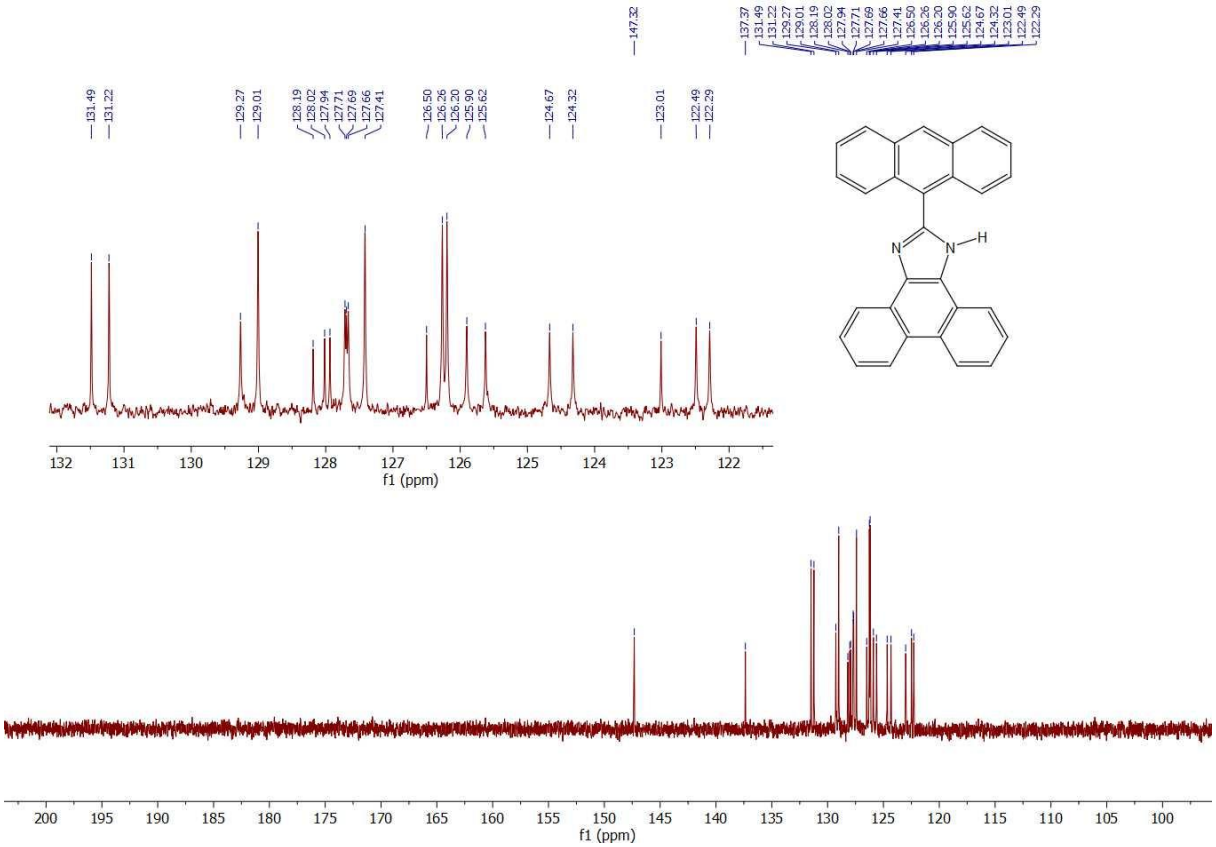

^{13}C NMR of 0E

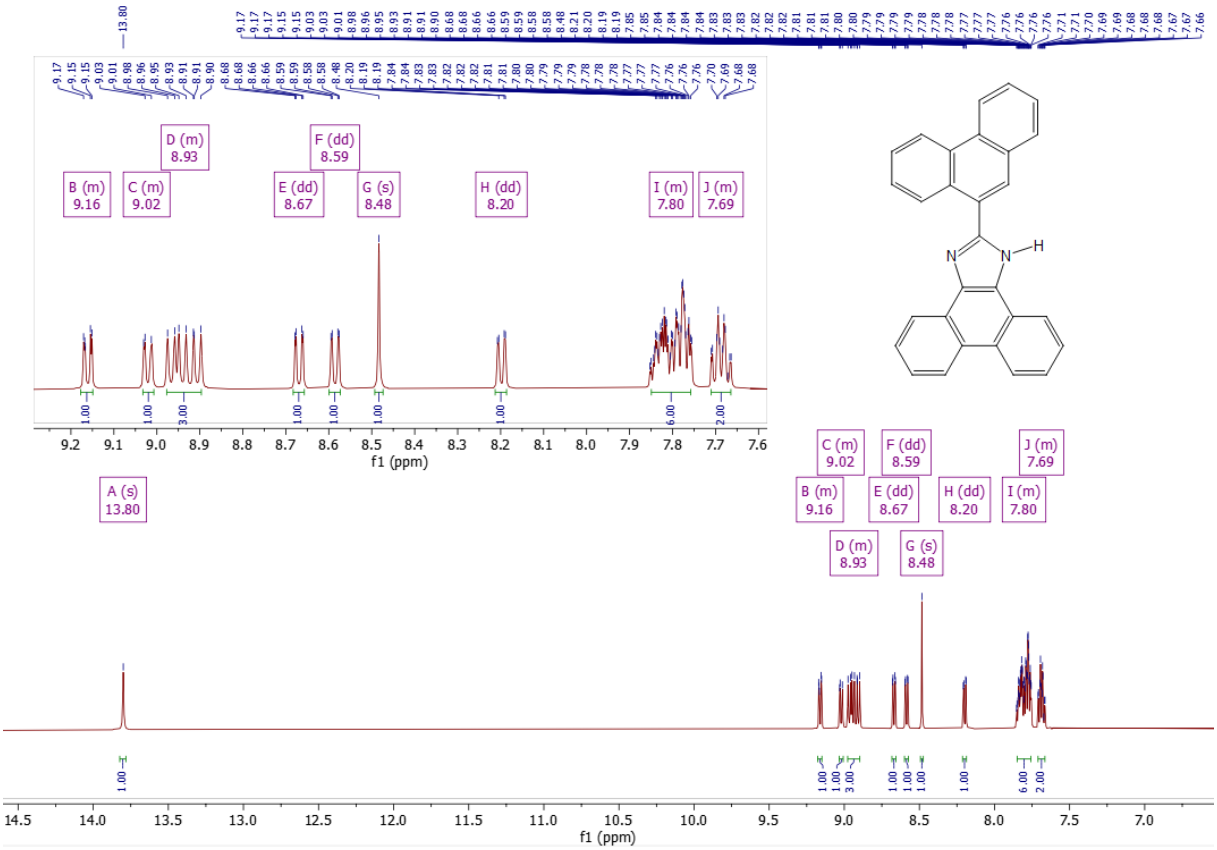

^{1}H NMR of 0F

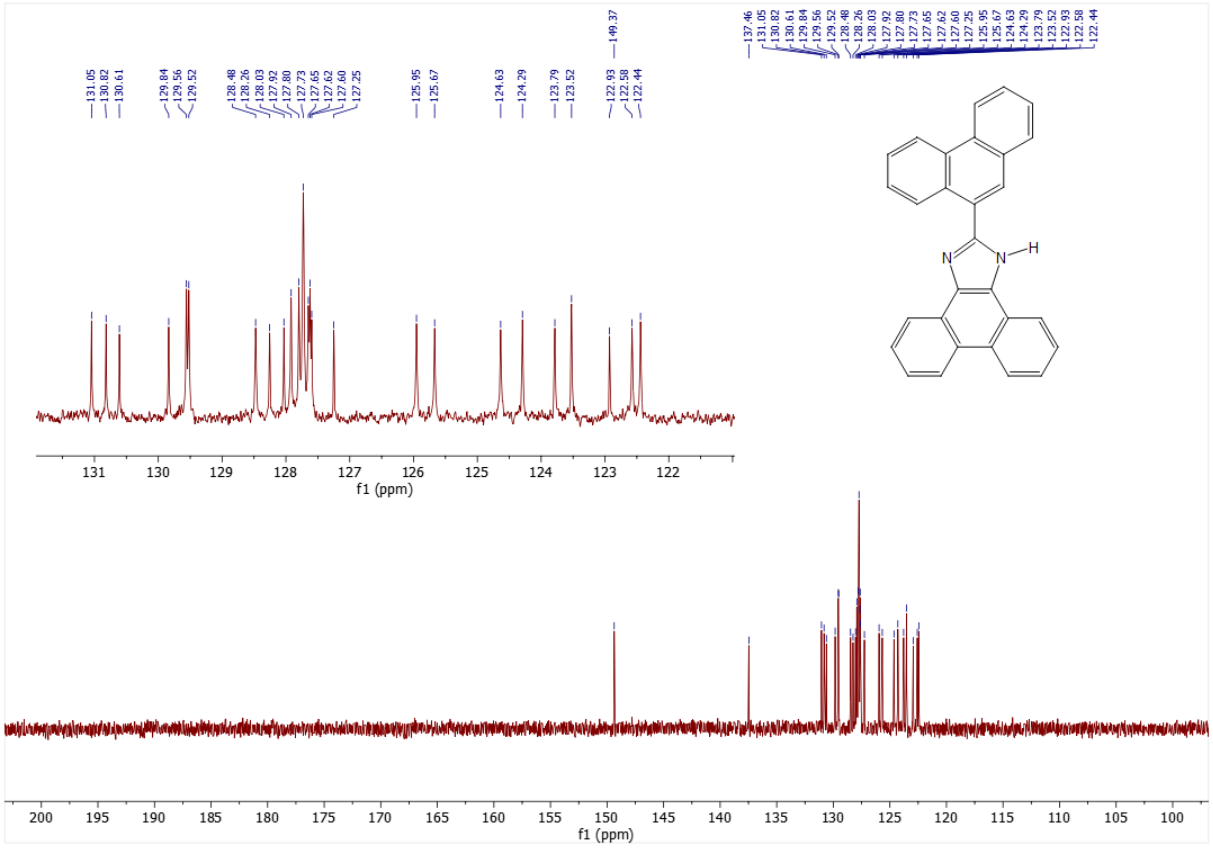

^{13}C NMR of 0F

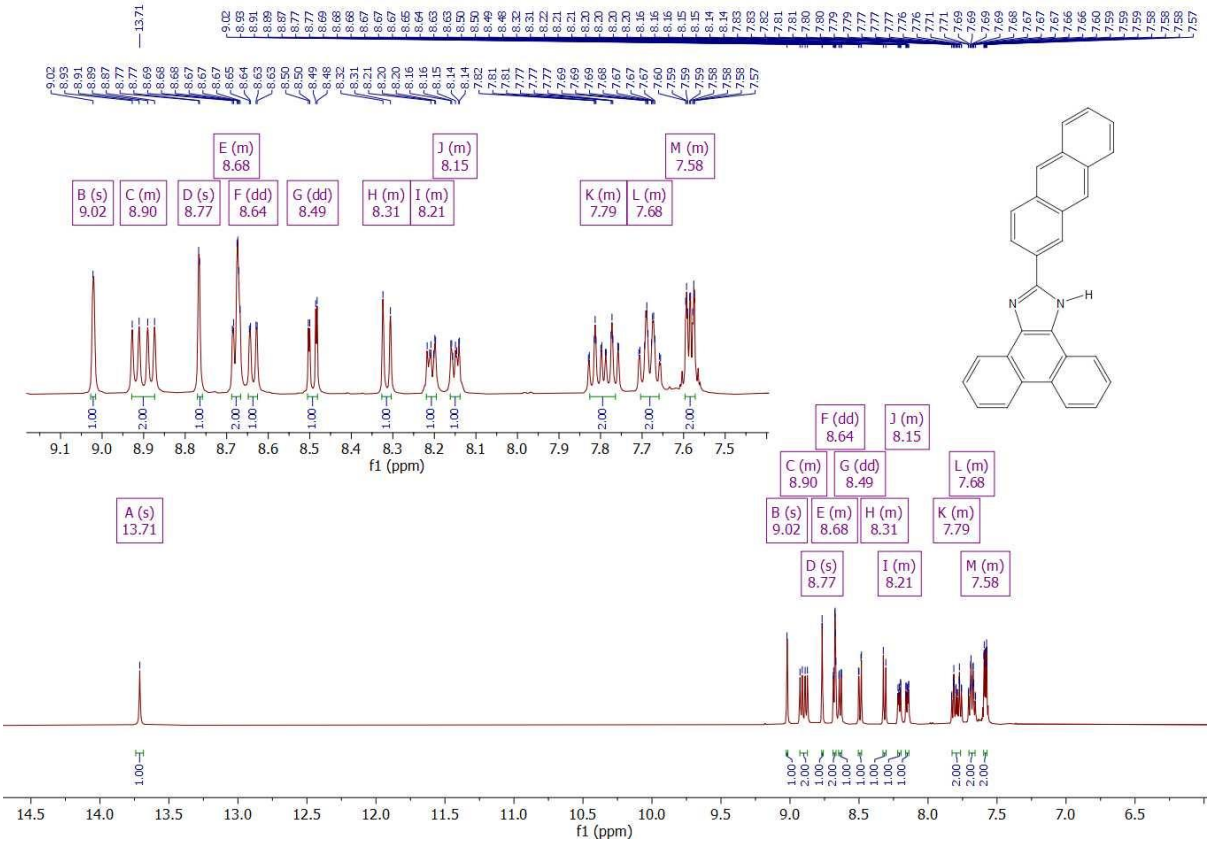

^{1}H NMR of 0G

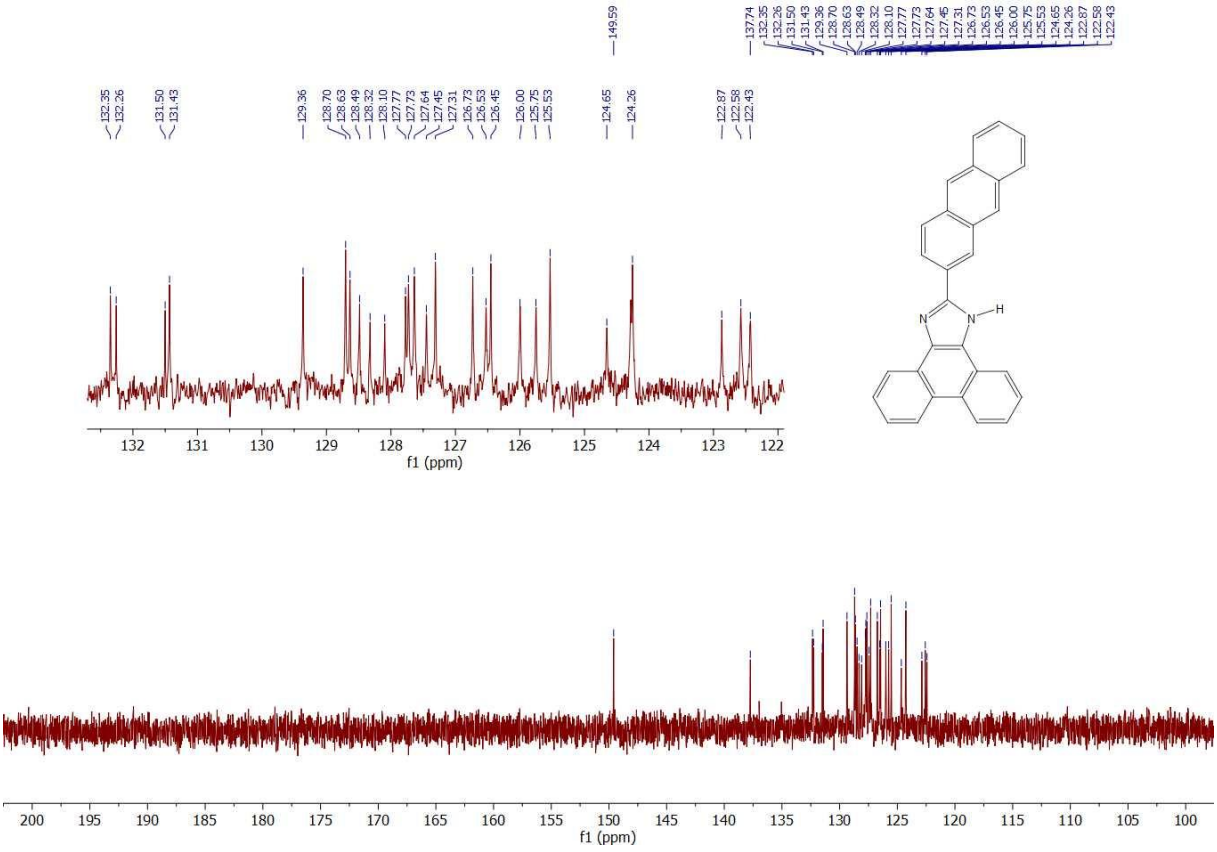

^{13}C NMR of 0G

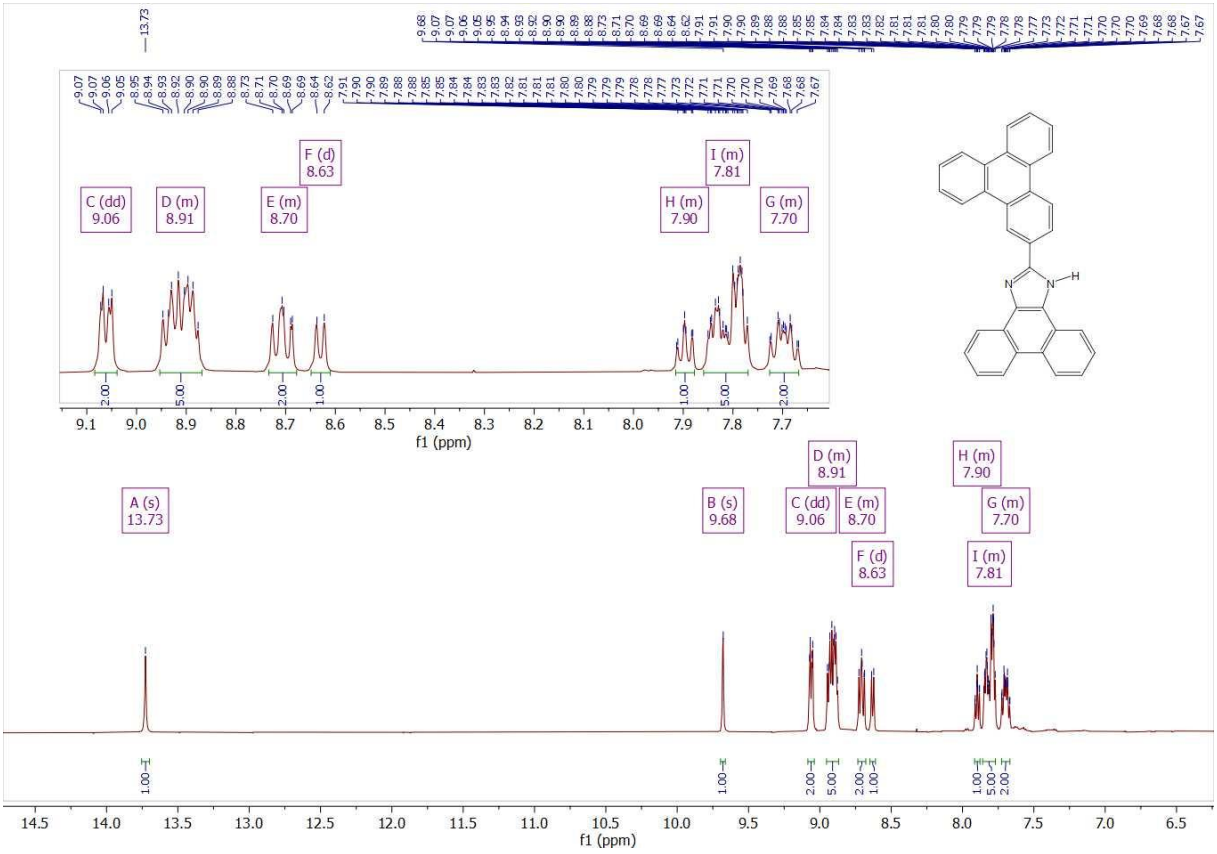

^{1}H NMR of 0H

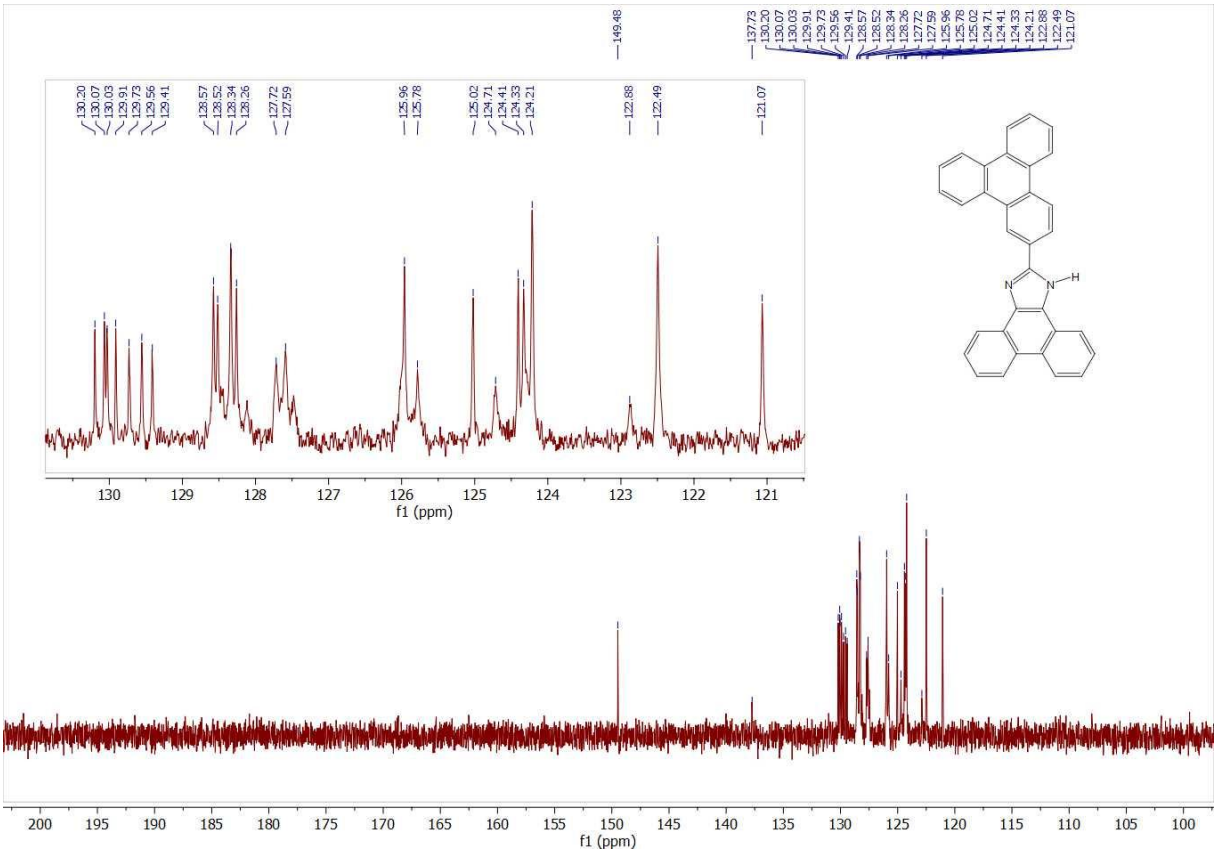

^{13}C NMR of 0H

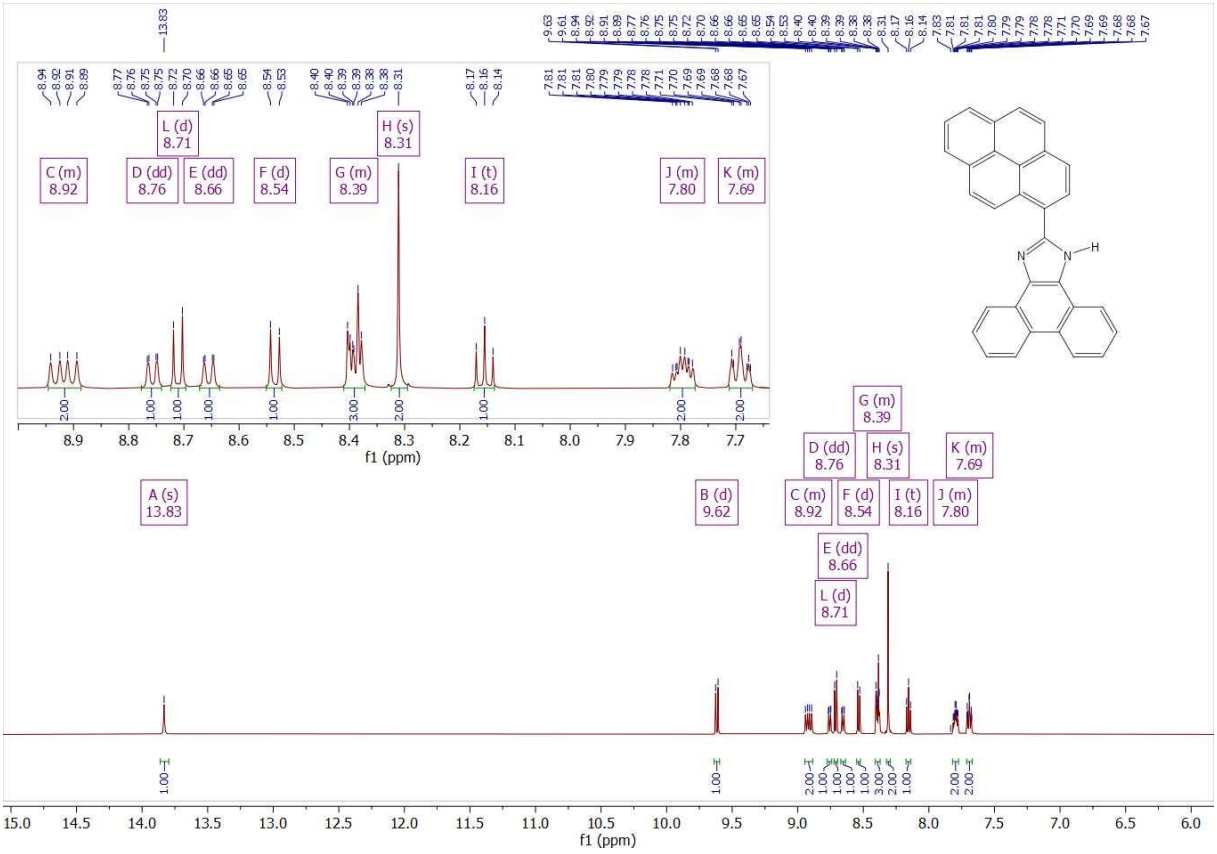

^{1}H NMR of 0I

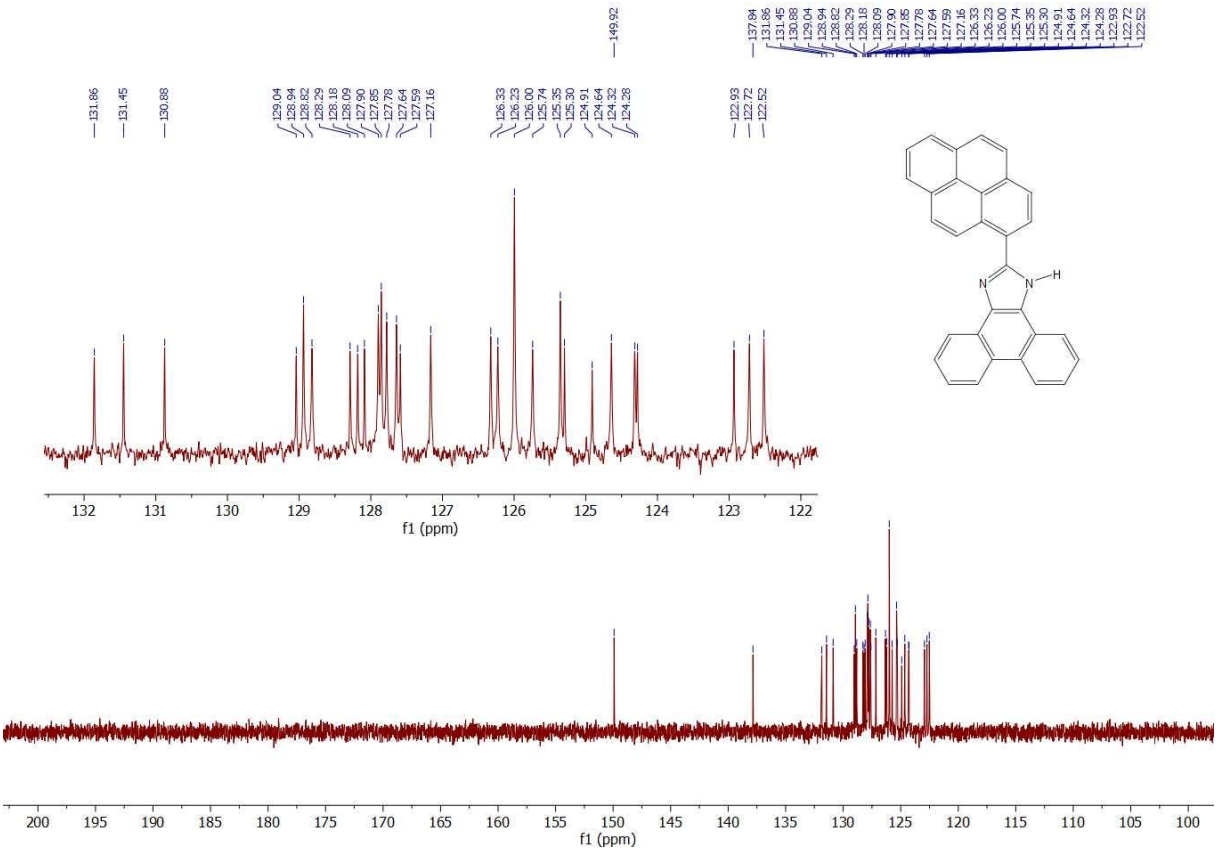

^{13}C NMR of 0I

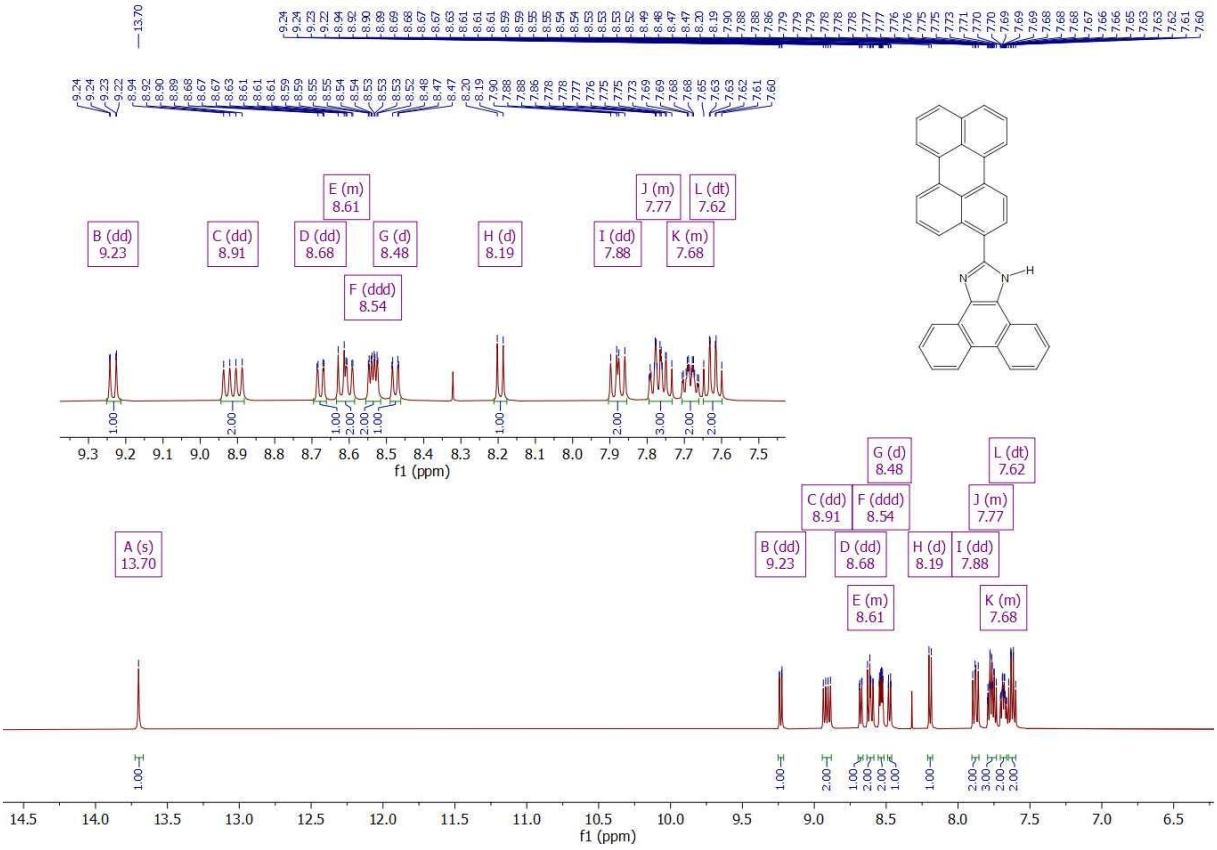

^{1}H NMR of 0J

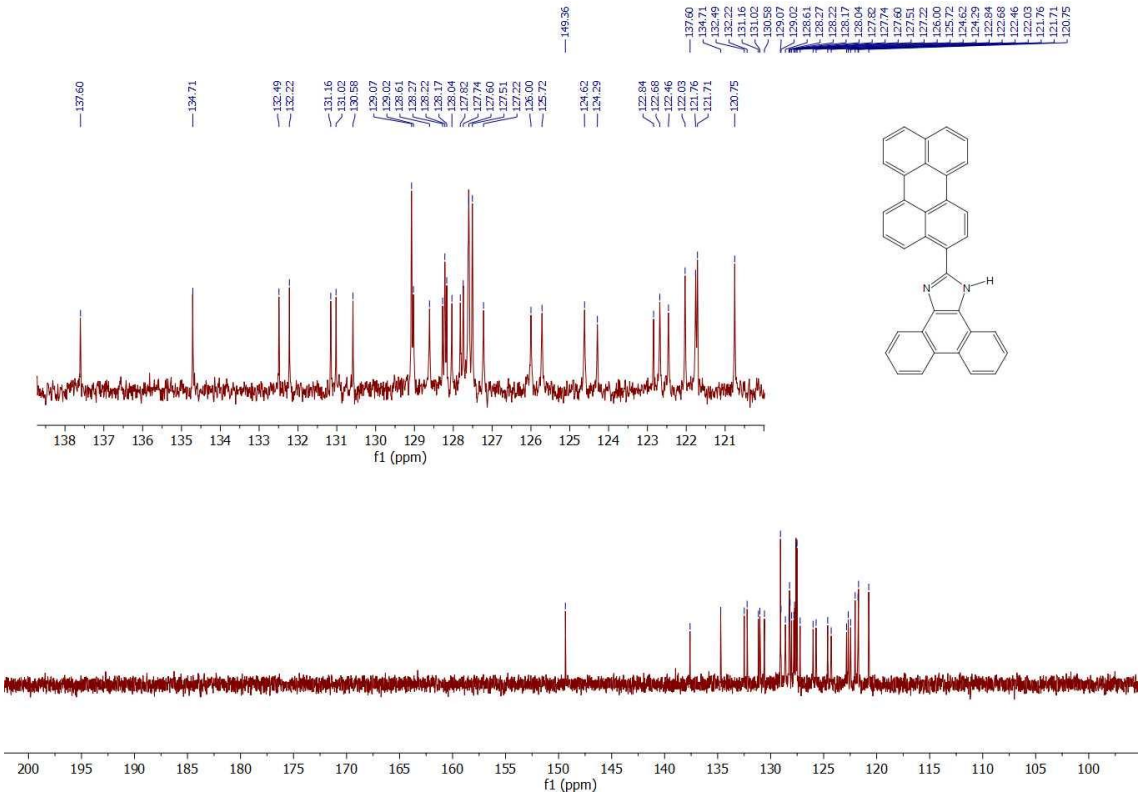

^{13}C NMR of 0J

HRMS of 0A

HRMS of 0B

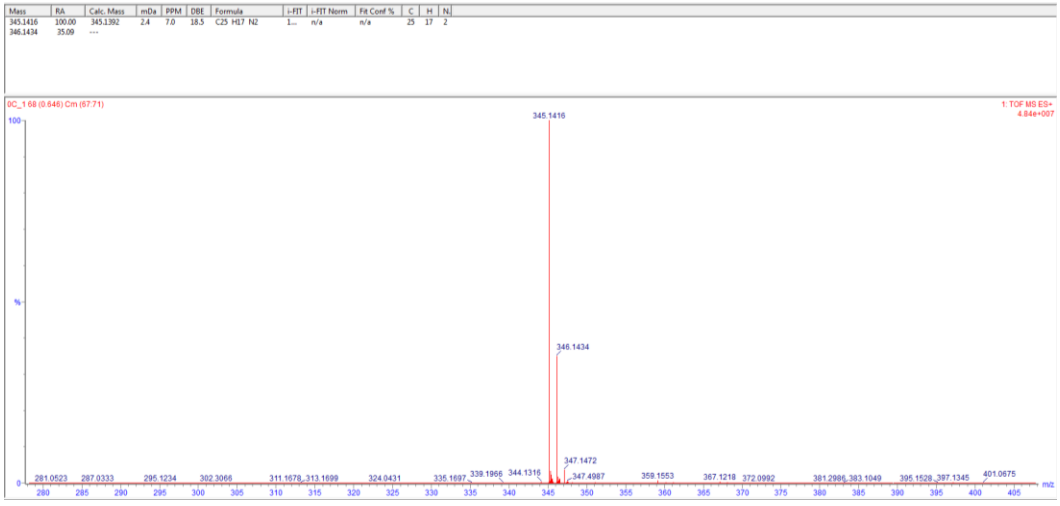

HRMS of 0C

HRMS of 0D

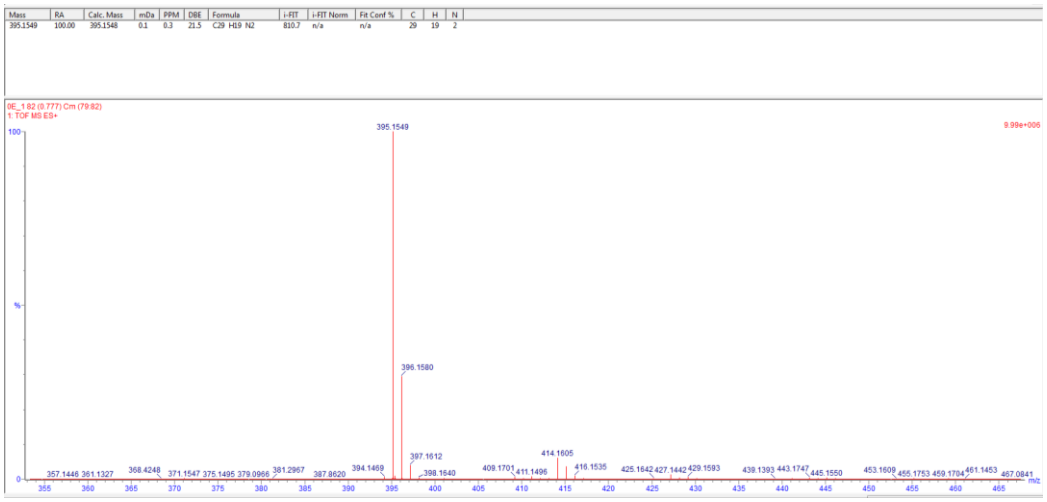

HRMS of 0E

HRMS of 0F

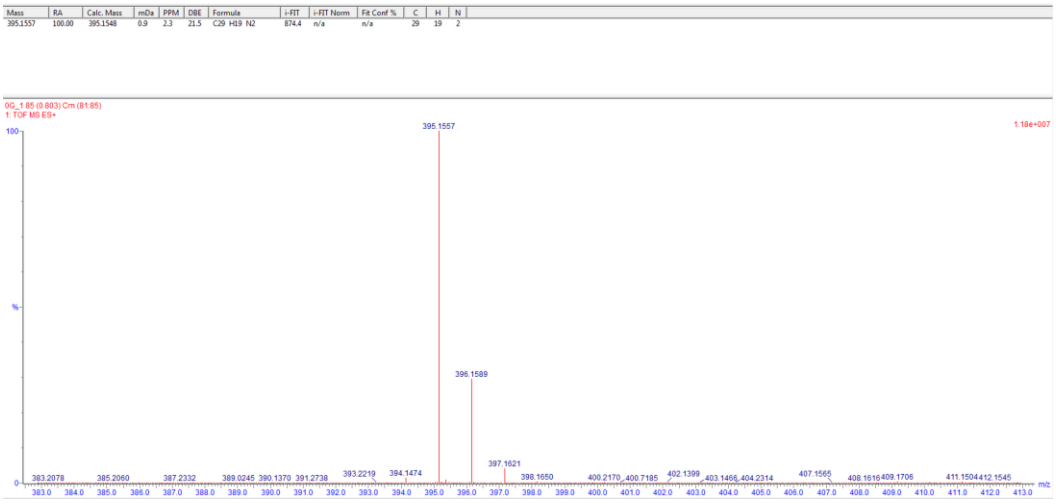

HRMS of 0G

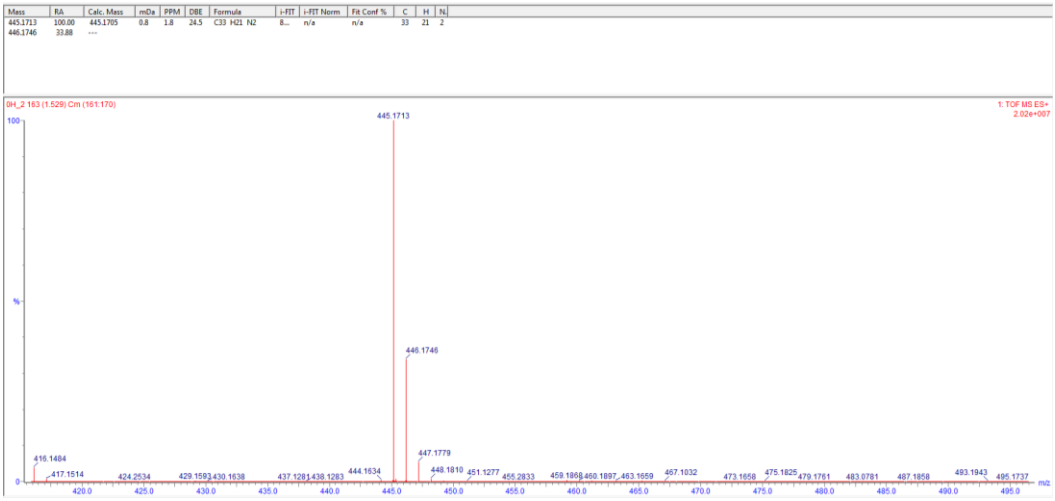

HRMS of 0H

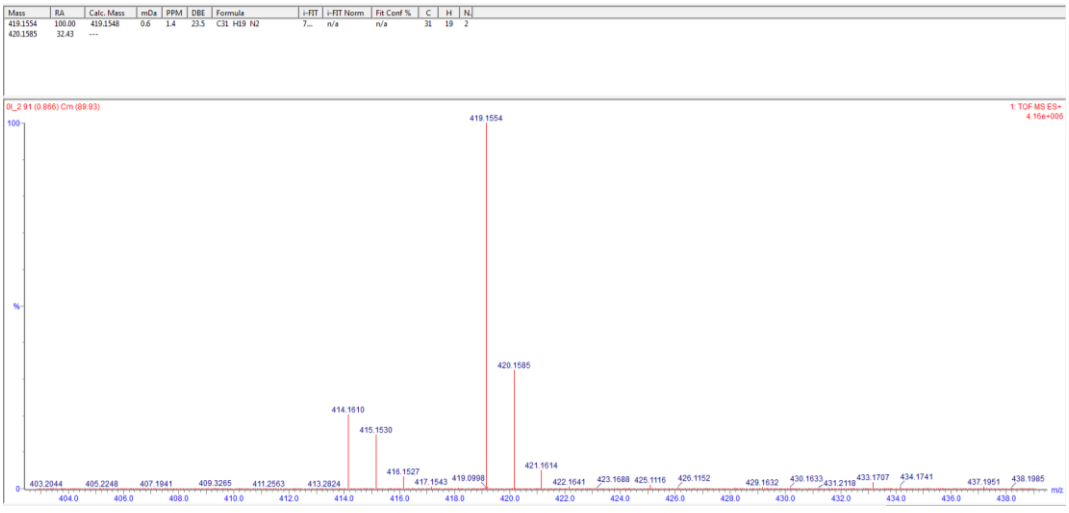

HRMS of 0I

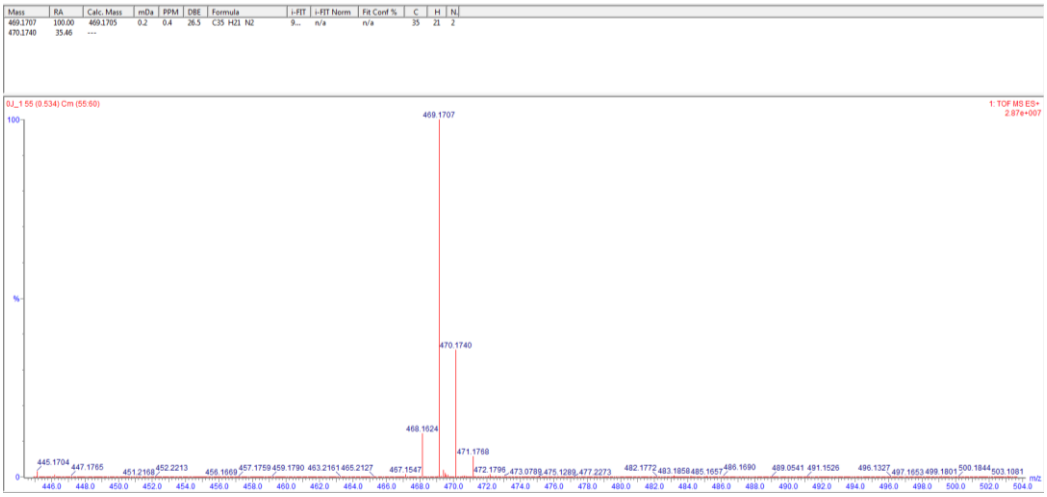
Mass RA Calc. Mass mDa PPM DBE Formula i-FIT i-FIT Norm Fit Conf % C H N
469.1707 100.00 469.1705 0.2 0.4 26.5 C35 H21 N2 9... n/a n/a 35 21 2
470.1740 35.46 ---
0J_1 55 (0.534) Cm (55:60)
1: TOF MS ES+
2.87e+007
100
%
0
469.1707
470.1740
468.1624
471.1768
445.1704
447.1765
451.2188
452.2213
456.1669
457.1759
459.1790
463.2161
465.2127
467.1547
472.1796
473.0789
475.1289
477.2273
482.1772
483.1858
485.1657
486.1690
489.0541
491.1526
496.1327
497.1653
499.1801
500.1844
503.1081
446.0 448.0 450.0 452.0 454.0 456.0 458.0 460.0 462.0 464.0 466.0 468.0 470.0 472.0 474.0 476.0 478.0 480.0 482.0 484.0 486.0 488.0 490.0 492.0 494.0 496.0 498.0 500.0 502.0 504.0
m/z

HRMS of 0J

5. Thermal properties

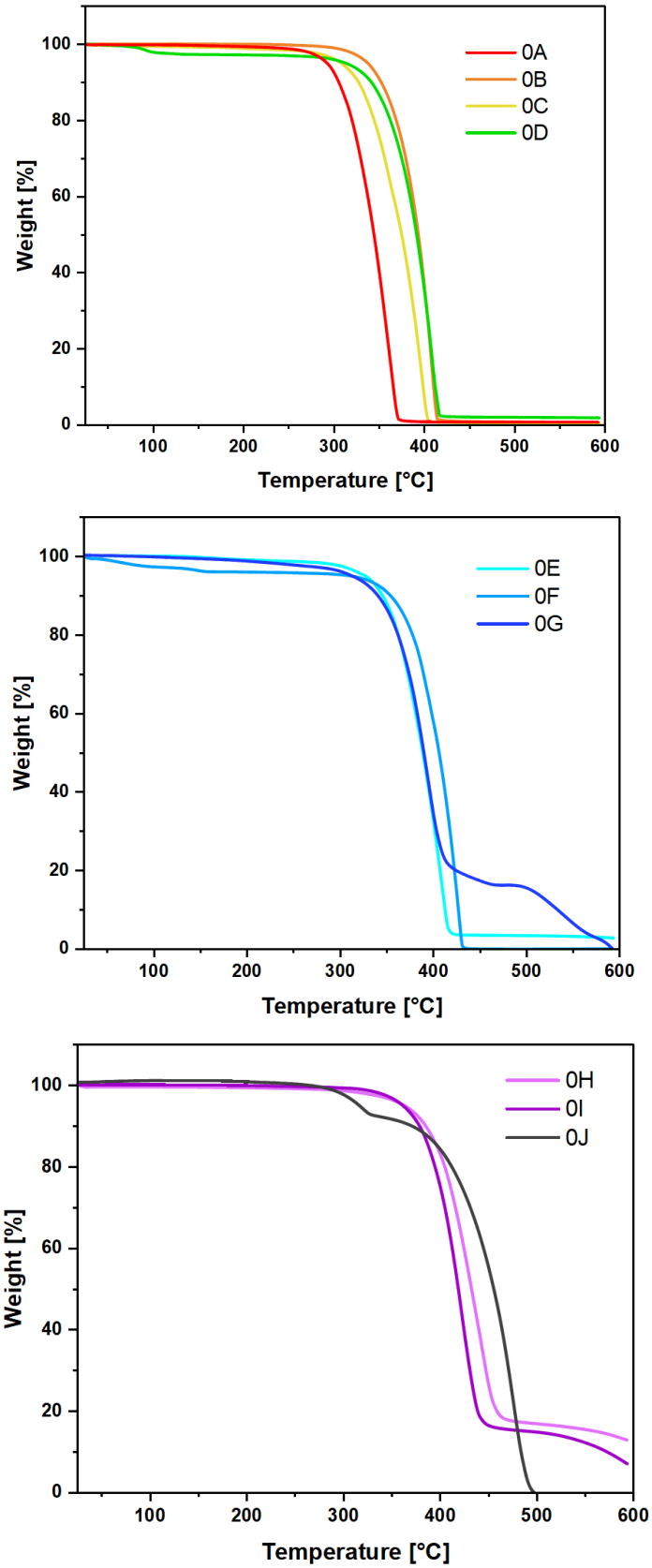

Figure S1. TGA thermograms – thermal properties of **0A**–**0J** series.

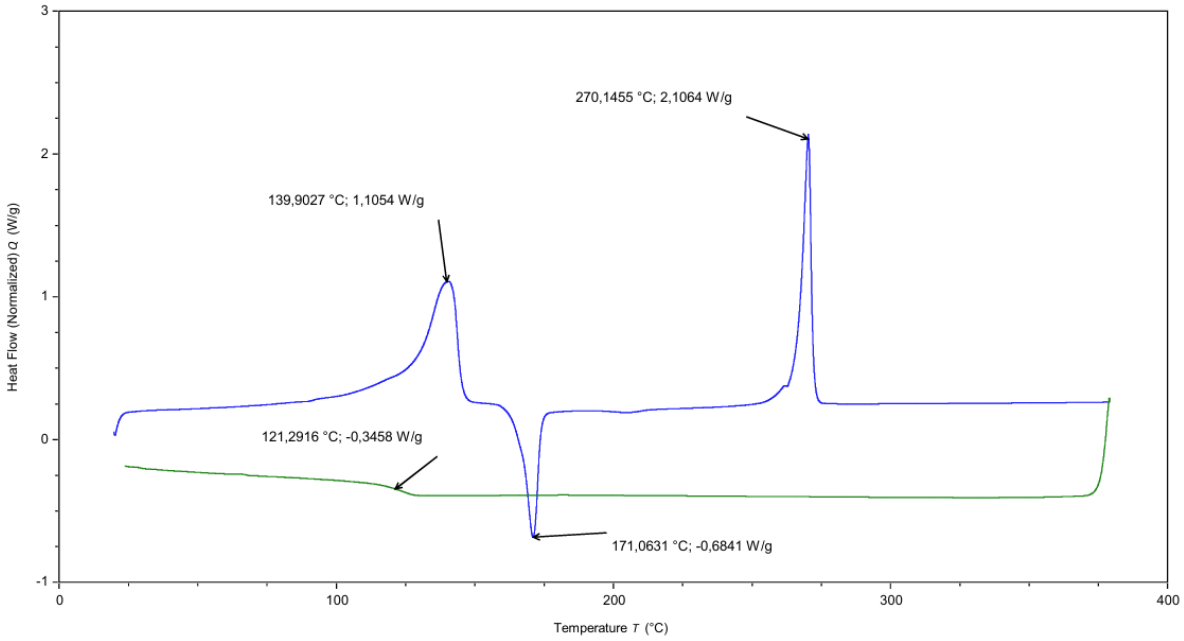

Figure S2. DSC thermograms of **0B**.

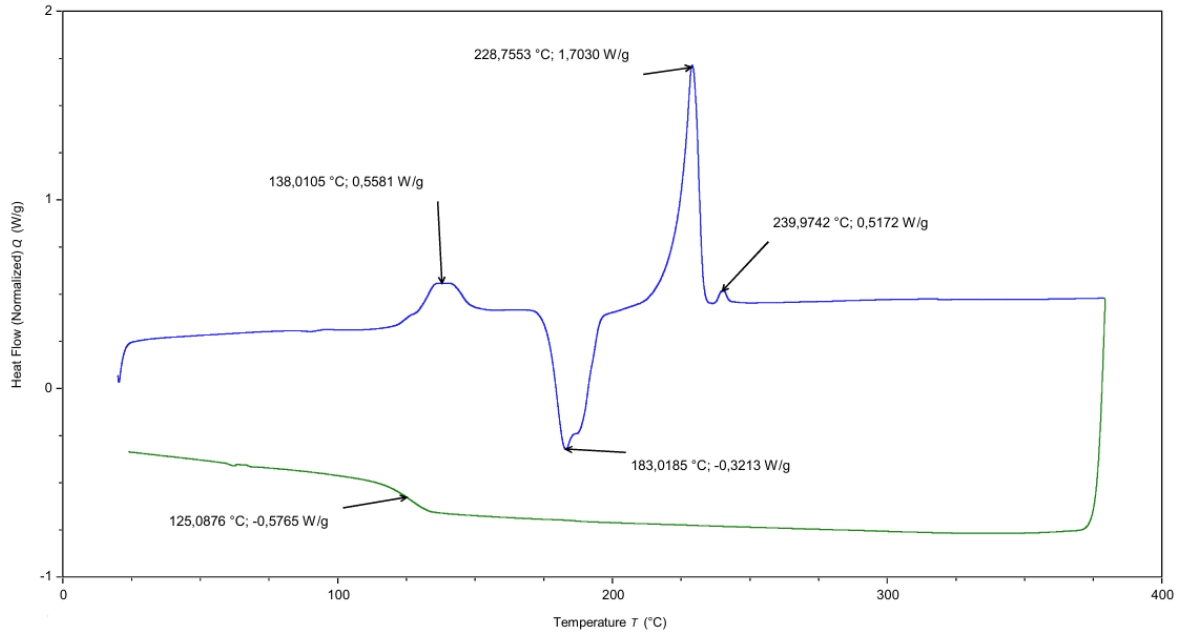

Figure S3. DSC thermograms of **0C**.

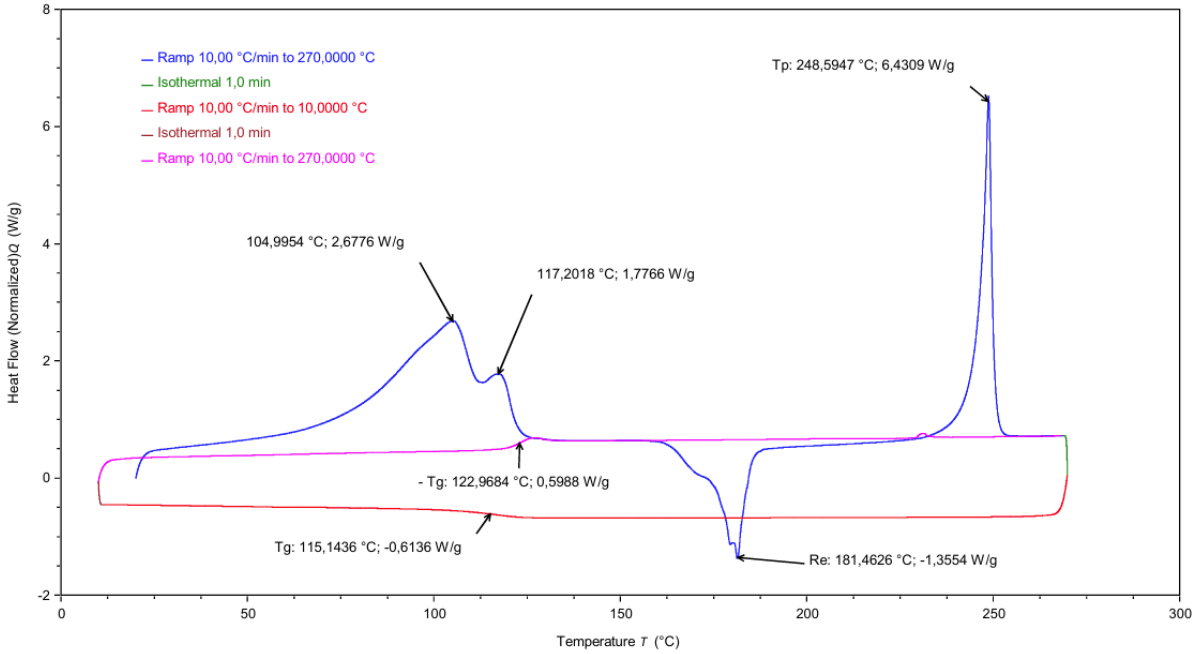

Figure S4. DSC thermograms of **0D**.

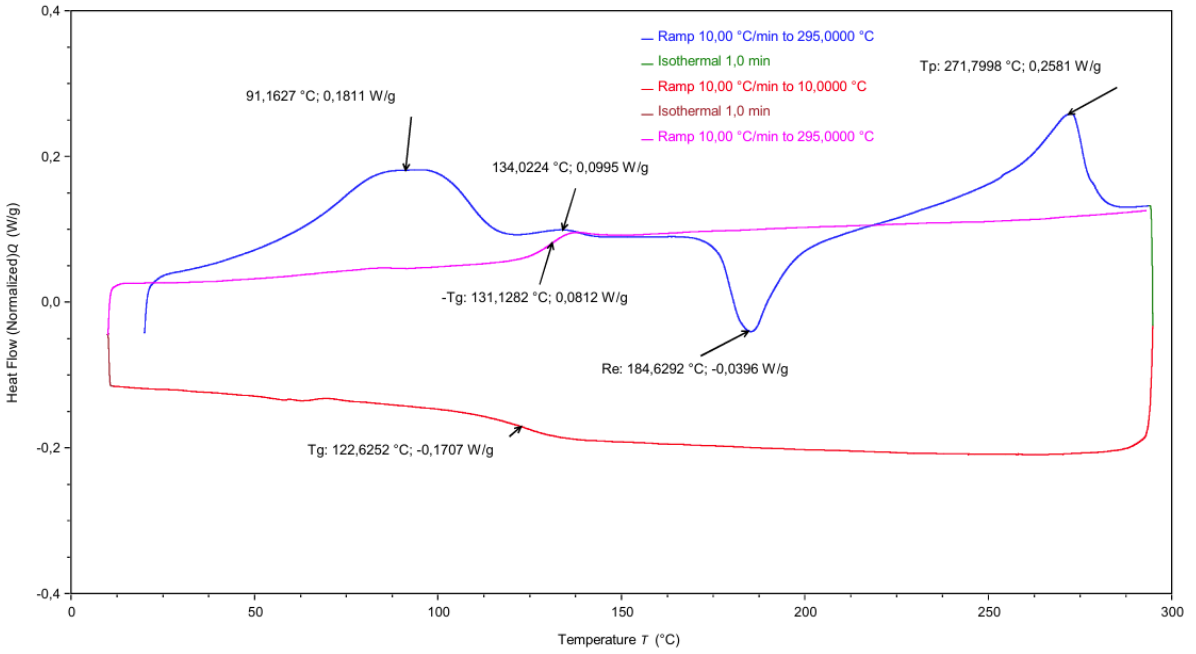

Figure S5. DSC thermograms of **0G**.

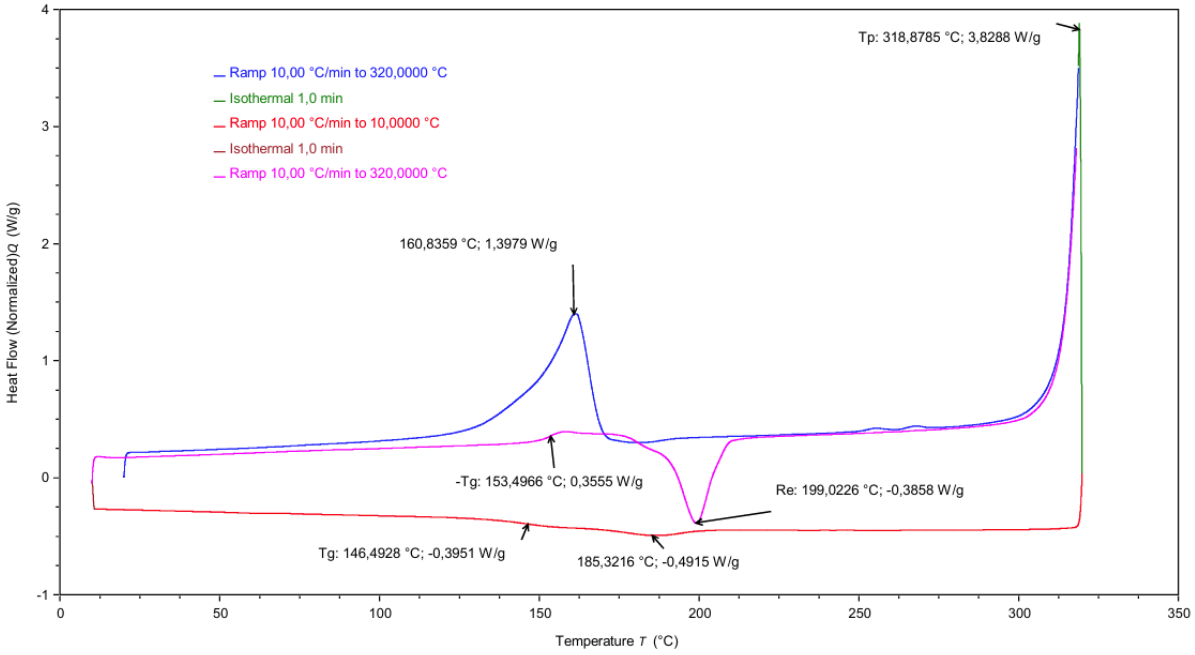

Figure S6. DSC thermograms of **0I**.

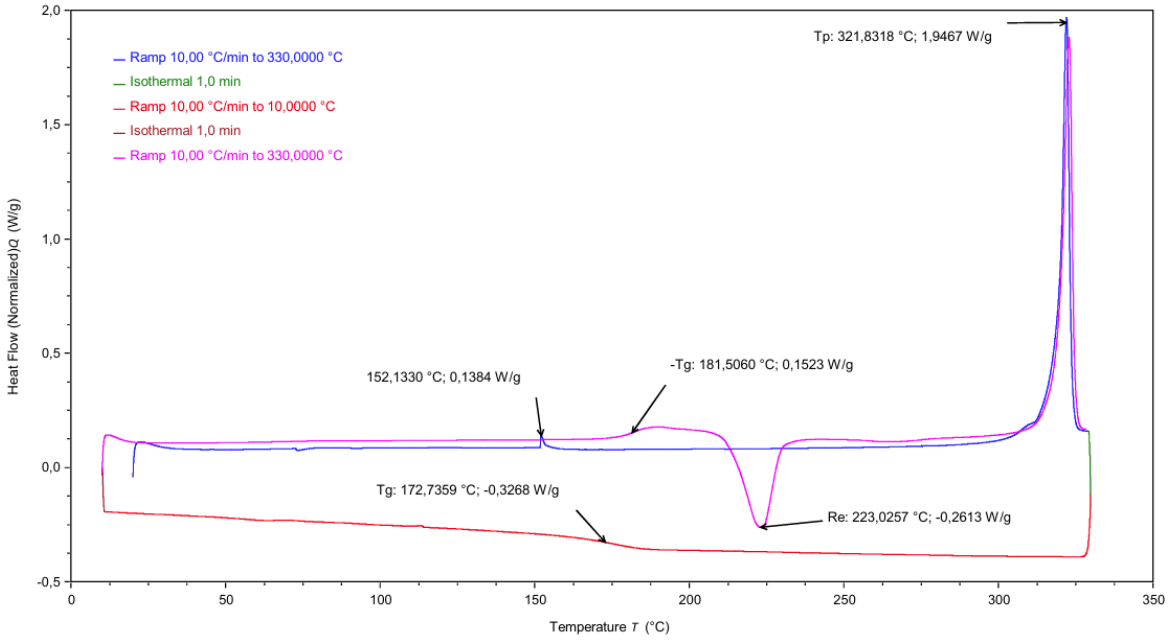

Figure S7. DSC thermograms of **0J**.

6. Electrochemical properties

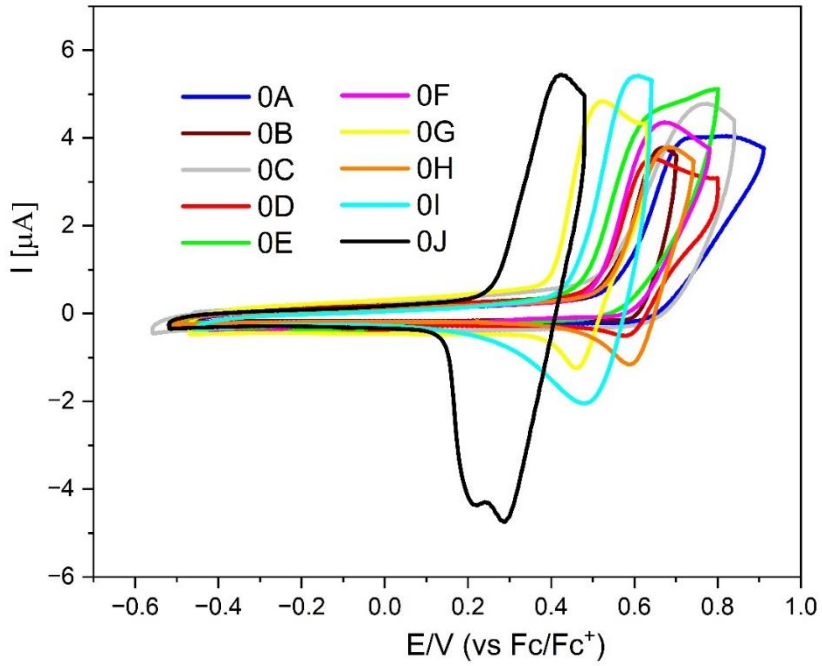

Figure S8. Cyclic voltammograms of the investigated compounds with sweep rate ν = 100 mV/s, 0.1 M Bu_4NPF_6 in CH_2Cl_2 during positive potential sweeping (c = 1 × 10^{-3} mol/L).

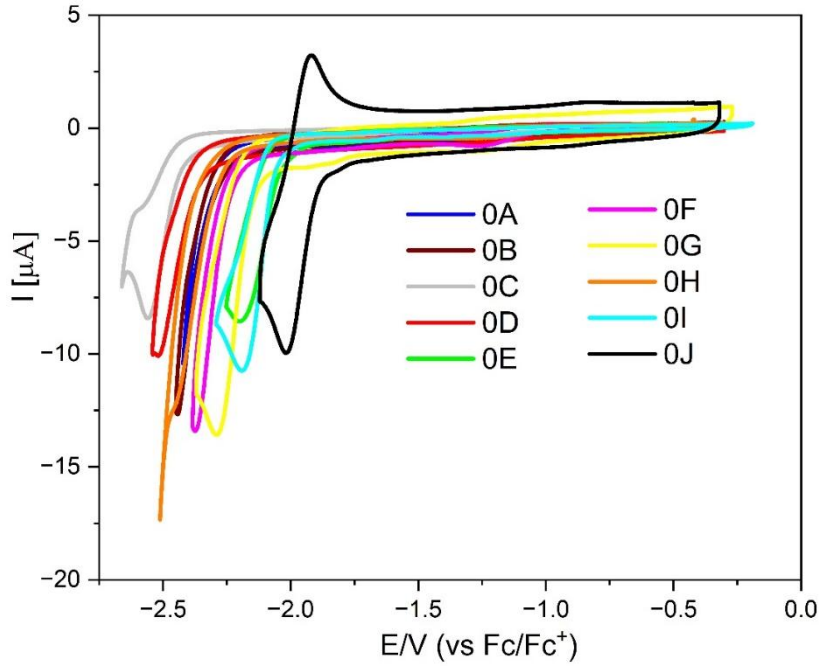

Figure S9. Cyclic voltammograms of the investigated compounds with sweep rate ν = 100 mV/s, 0.1 M Bu_4NPF_6 in CH_2Cl_2 during negative potential sweeping (c = 1 × 10^{-3} mol/L).

7. DFT calculations

0A	0B
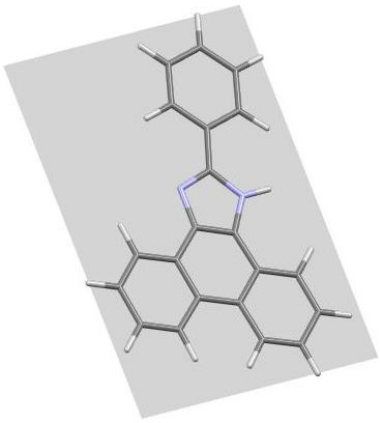	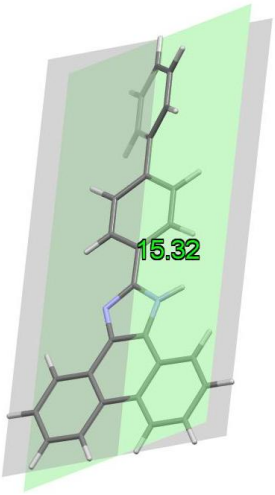
0C	**0D**
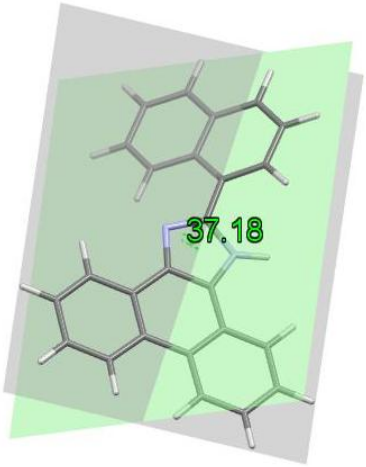	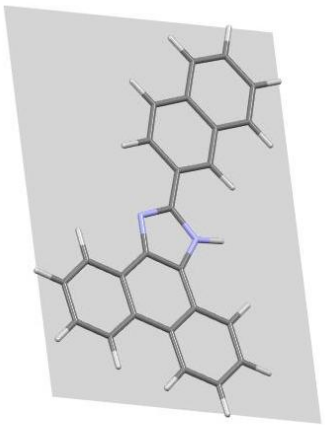
0E	**0F**
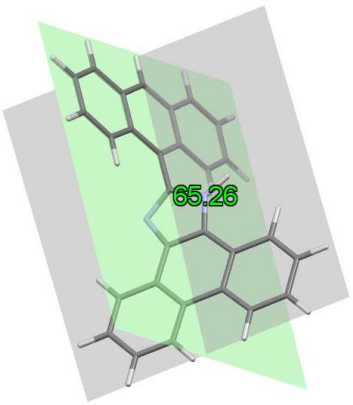	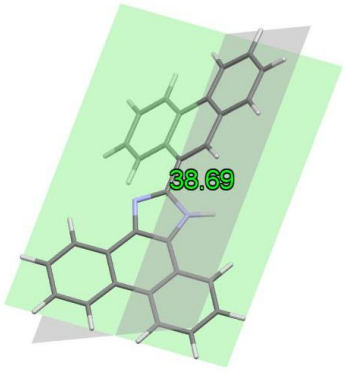

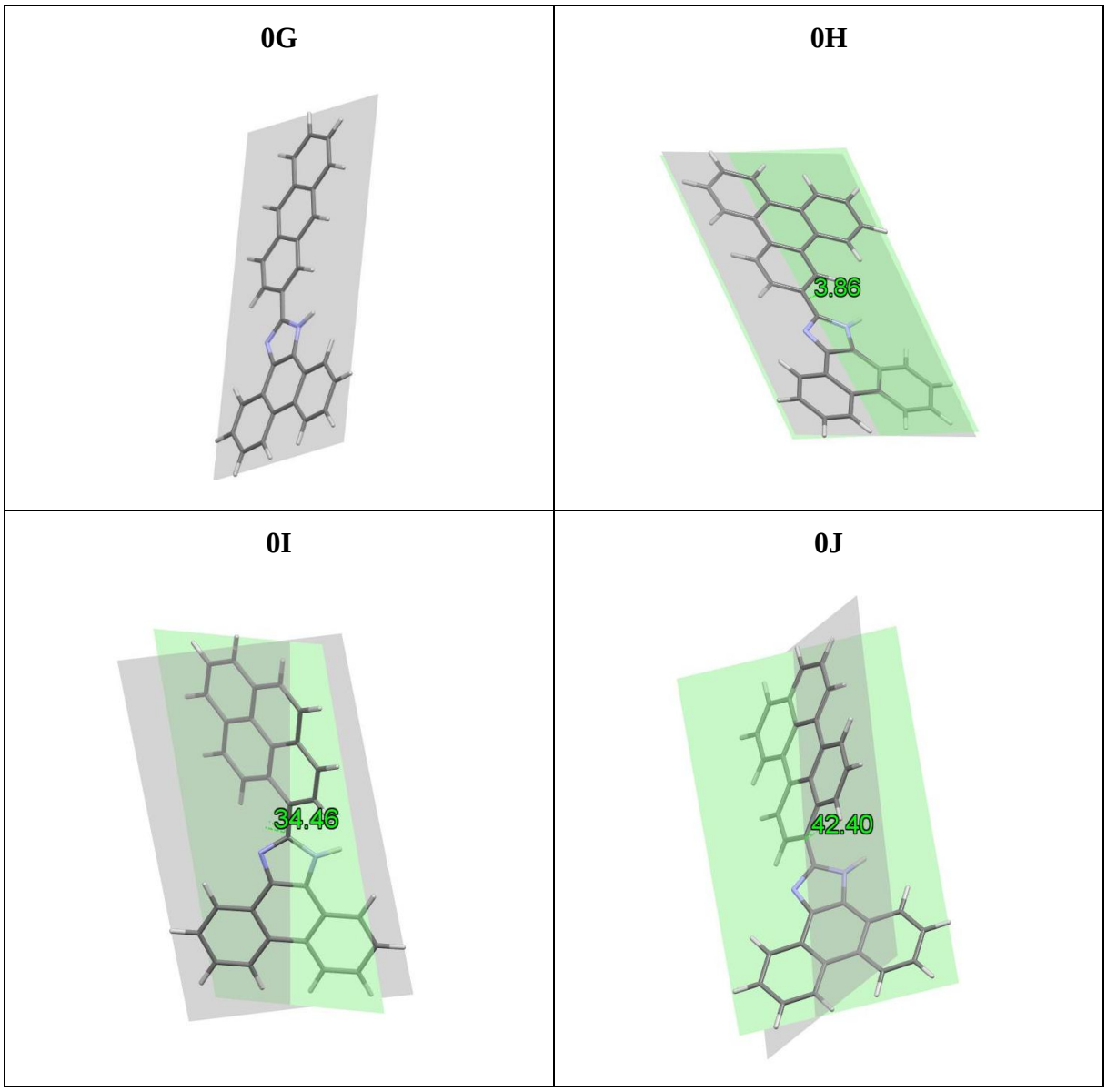

Figure S10. Dihedral angle between the plane of the aromatic group and the central core of 1H-phenanthro[9,10-d]imidazole for derivatives **0A**–**0J**.

Table S1. Calculated ionization potentials and electron affinities (vertical and adiabatic), energy gap, hole and electron reorganization energies and extraction potentials.

Compound	IP_v [eV]	IP_a [eV]	EA_v [eV]	EA_a [eV]	$\lambda_{electron}$ [eV]	λ_{hole} [eV]	λ_{hole} - $\lambda_{electron}$ [eV]	HEP [eV]	EEP [eV]
0A	5.72	5.61	1.60	1.76	0.31	0.21	0.10	5.51	1.92
0B	5.66	5.55	1.82	2.02	0.38	0.22	0.16	5.45	2.20
0C	5.71	5.58	1.84	2.07	0.42	0.26	0.16	5.45	2.26
0D	5.57	5.57	1.89	2.03	0.27	0.10	0.17	5.47	2.16
0E	5.67	5.48	2.29	2.43	0.29	0.19	0.10	5.48	2.58
0F	5.72	5.59	1.88	2.12	0.44	0.13	0.31	5.59	2.32
0G	5.54	5.46	2.33	2.43	0.20	0.17	0.03	5.38	2.53
0H	5.67	5.56	1.93	2.07	0.27	0.24	0.03	5.43	2.20
0I	5.54	5.42	2.21	2.36	0.30	0.24	0.06	5.31	2.50
0J	5.36	5.25	2.57	2.69	0.23	0.22	0.01	5.14	2.80

$EEP = E^0(M^-) - E^-(M^-)$; $HEP = E^+(M^+) - E^0(M^+)$; $\lambda_{electron} = EEP - EA_v$; $\lambda_{hole} = IP_v - HEP$

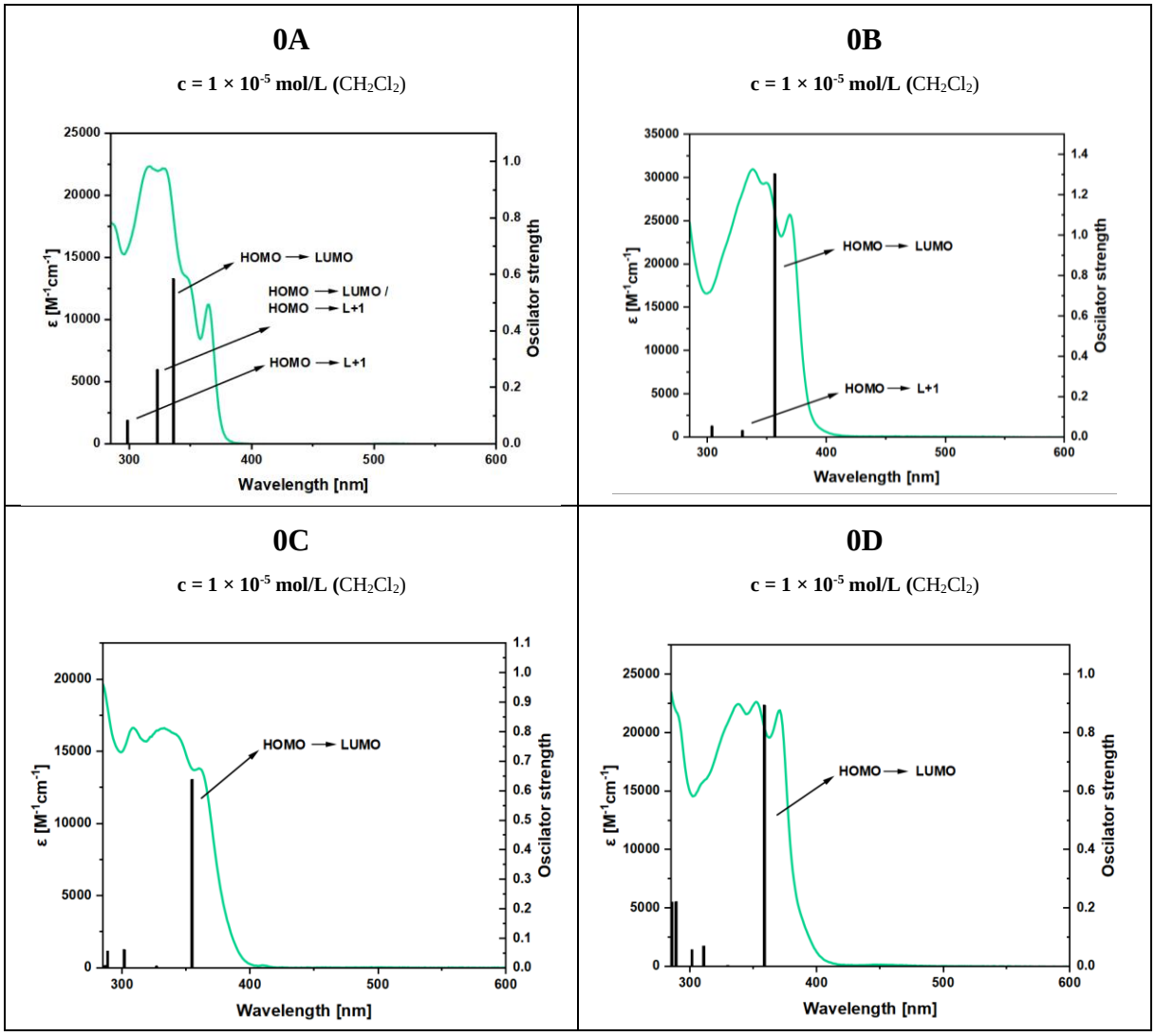

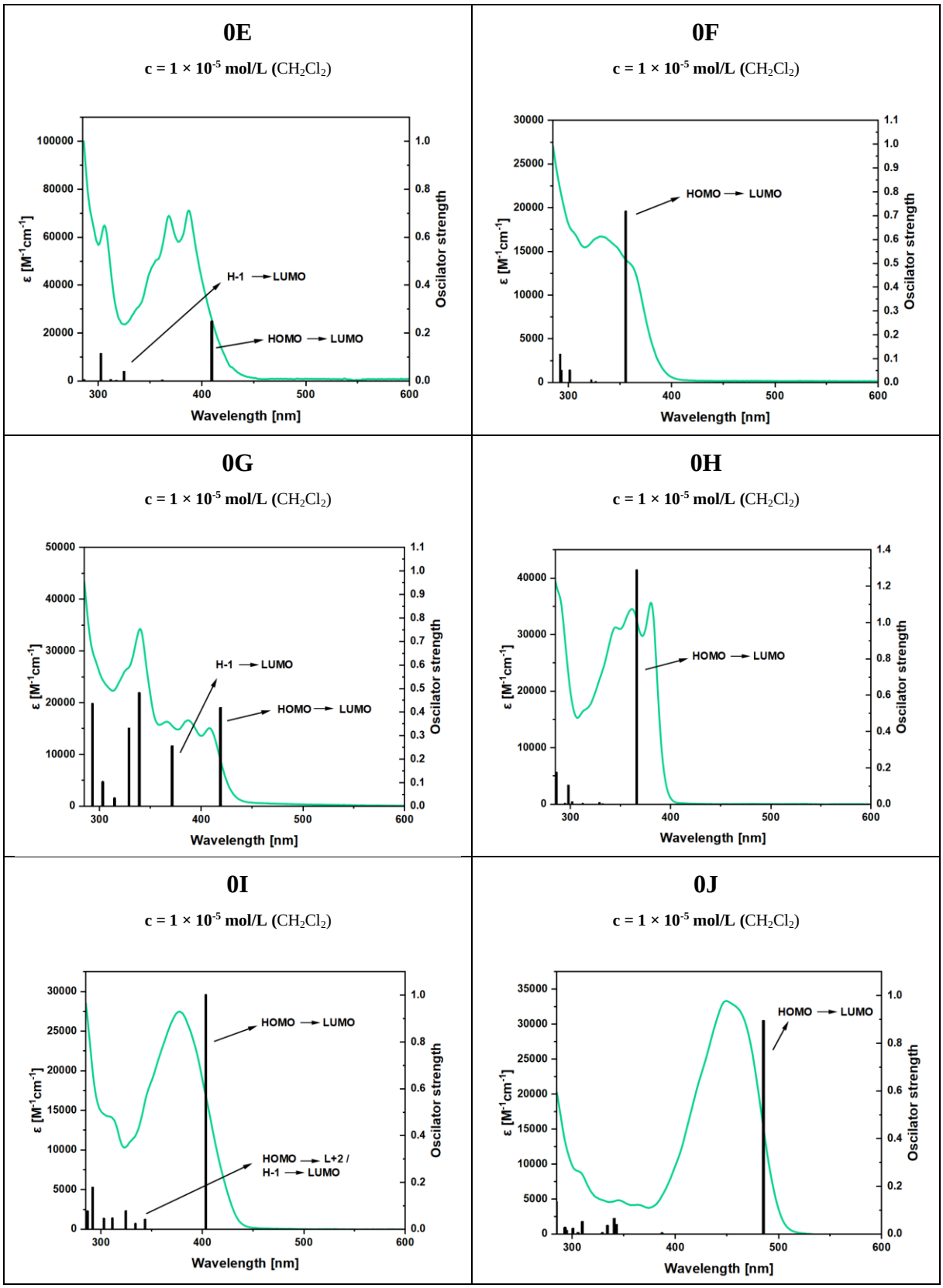

Figure S11. Experimental (green line) absorption spectra and calculated transitions (black sticks) of **0A**–**0J** in CH_2Cl_2.

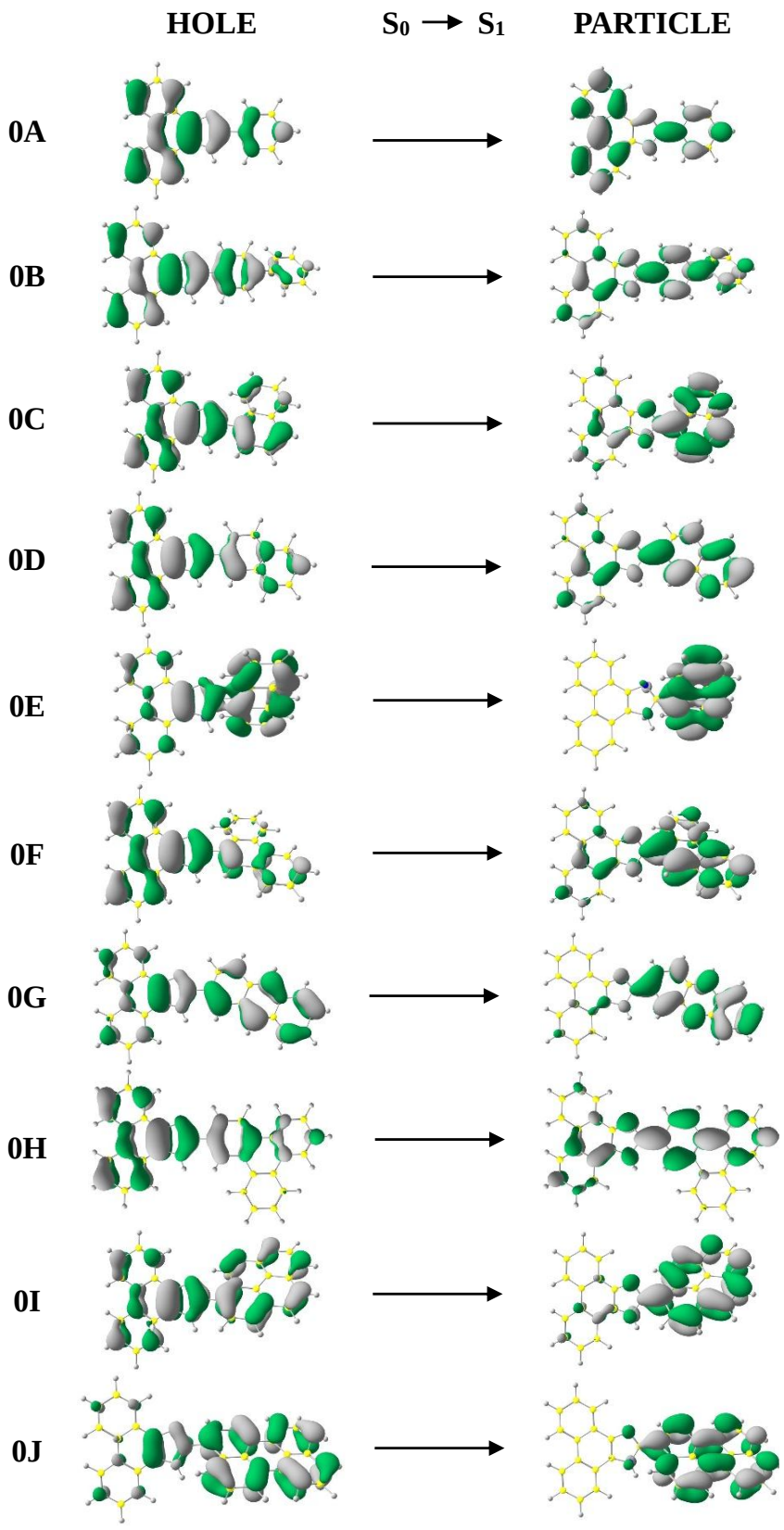

Figure S12. The $S_0 \rightarrow S_1$ transition NTO.

8. Optical properties

0A – absorption normalized

c = 1 × 10^{-5} mol/L

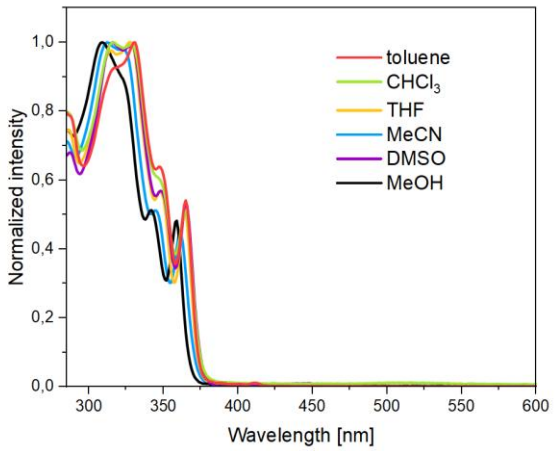

0A – emission

c = 1 × 10^{-5} mol/L; $\lambda_{excitation}$ = 340 nm

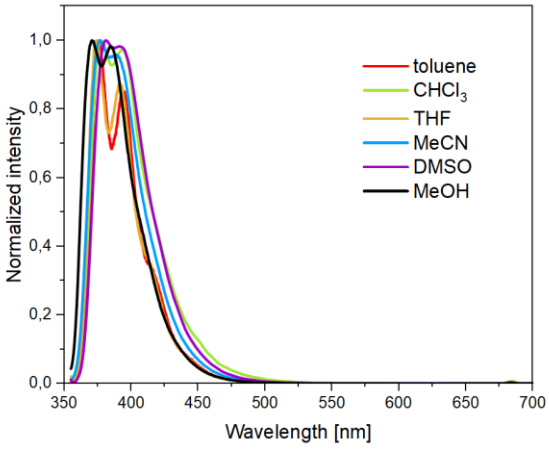

0A – absorption

c = 1 × 10^{-5} mol/L

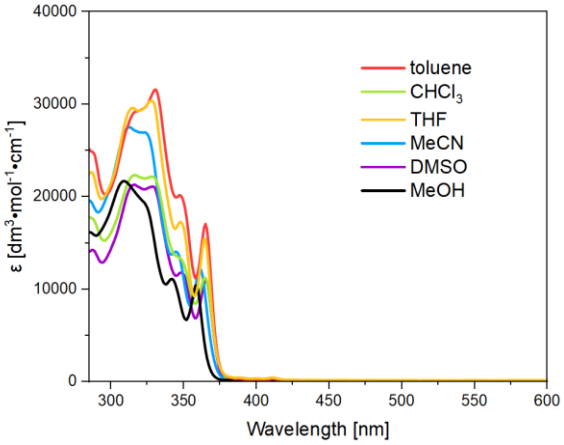

0A – aggregation

c = 1 × 10^{-5} mol/L; $\lambda_{excitation}$ = 340 nm

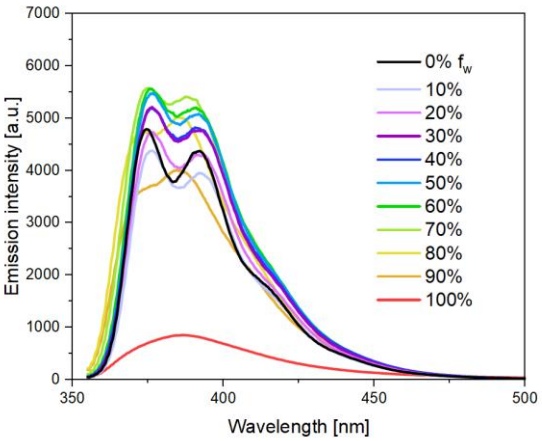

0B – absorption normalized

c = 1 × 10^{-5} mol/L

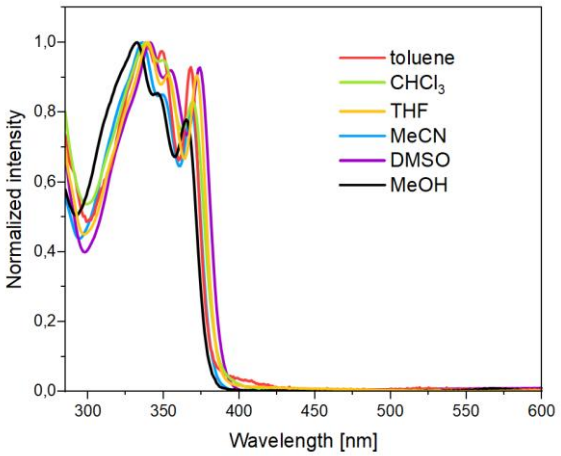

0B – emission

c = 1 × 10^{-5} mol/L; $\lambda_{excitation}$ = 360 nm

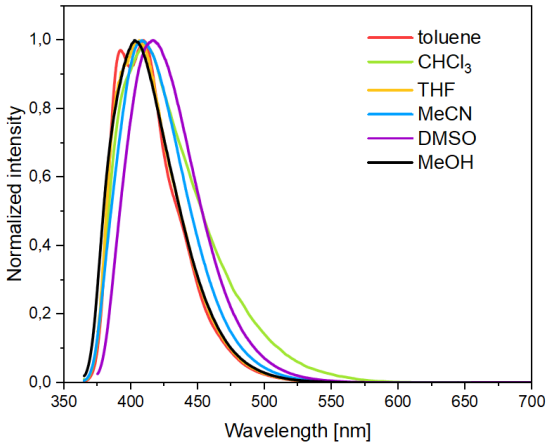

0B – absorption

c = 1 × 10^{-5} mol/L

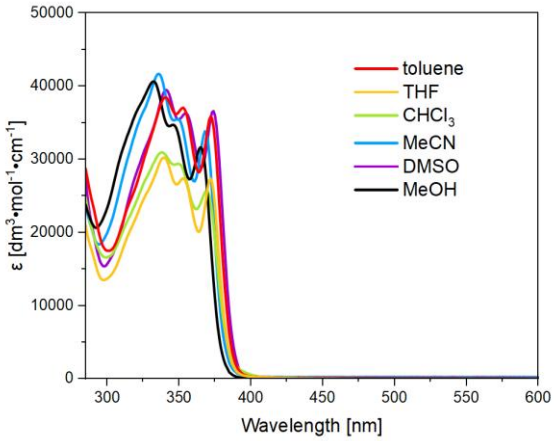

0B – aggregation

c = 1 × 10^{-5} mol/L; $\lambda_{excitation}$ = 360 nm

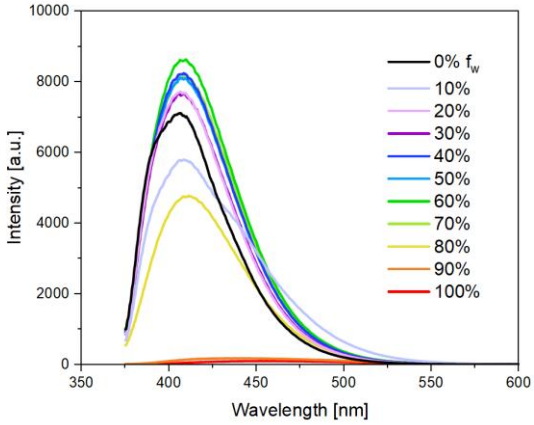

0C – absorption normalized

c = 1 × 10^{-5} mol/L

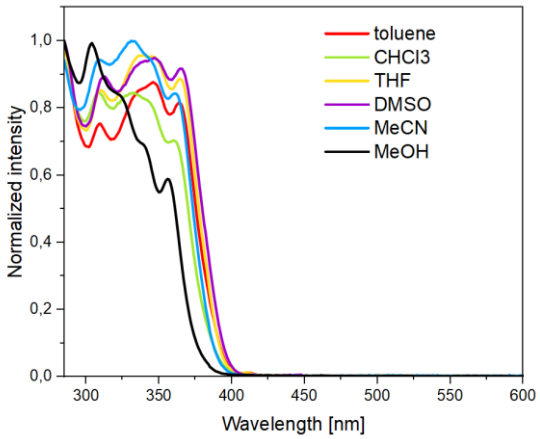

0C – emission

c = 1 × 10^{-5} mol/L; $\lambda_{excitation}$ = 360 nm

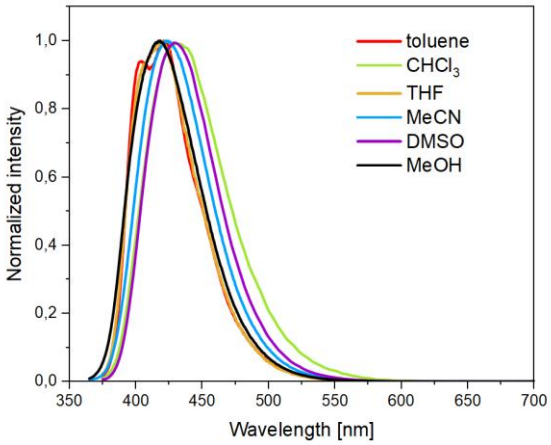

0C – absorption

c = 1 × 10^{-5} mol/L

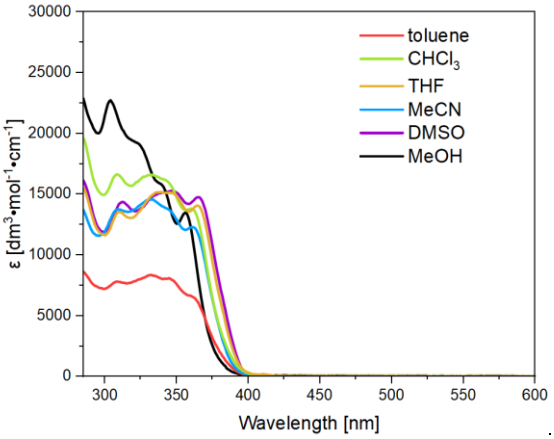

0C – aggregation

c = 1 × 10^{-5} mol/L; $\lambda_{excitation}$ = 360 nm

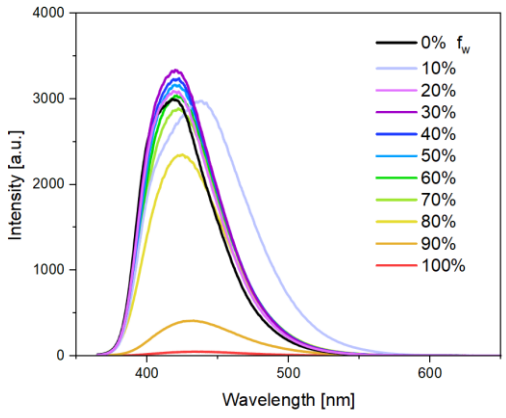

0D – absorption normalized

c = 1 × 10^{-5} mol/L

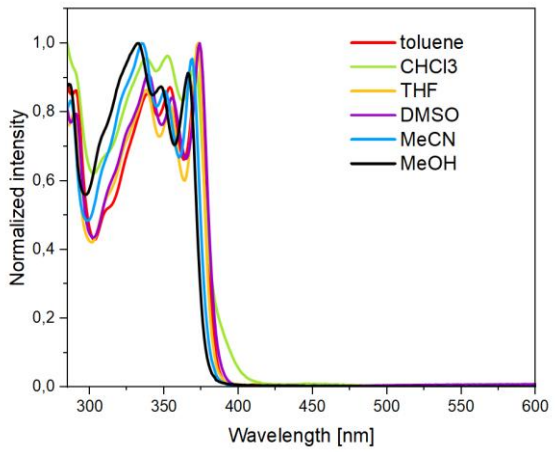

0D – emission

c = 1 × 10^{-5} mol/L; $\lambda_{excitation}$ = 350 nm

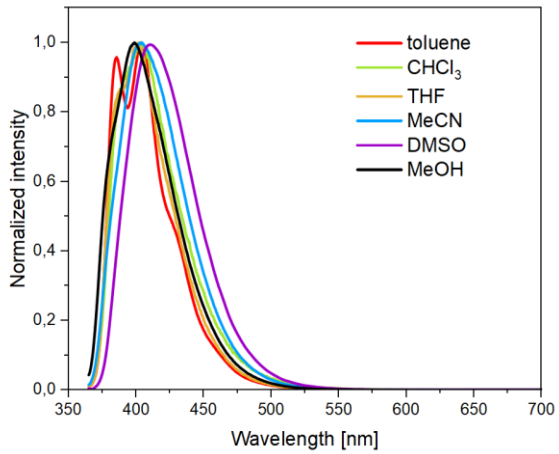

0D – absorption

c = 1 × 10^{-5} mol/L

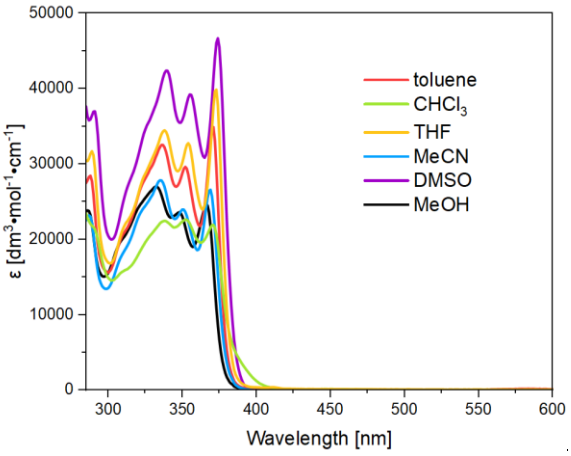

0D – aggregation

c = 1 × 10^{-5} mol/L; $\lambda_{excitation}$ = 350 nm

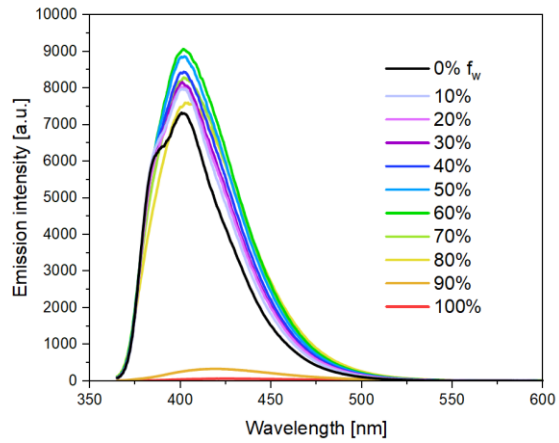

0E – absorption normalized

c = 1 × 10^{-5} mol/L

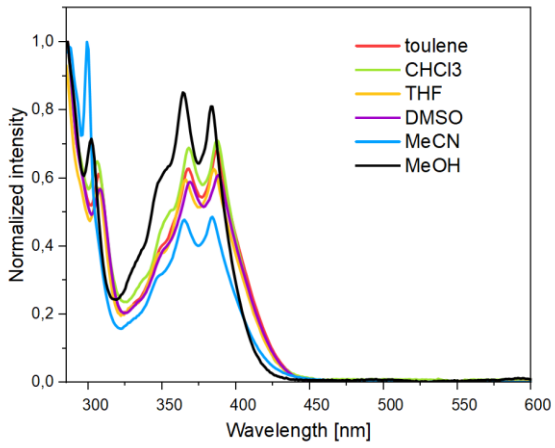

0E – emission

c = 1 × 10^{-5} mol/L; $\lambda_{excitation}$ = 380 nm

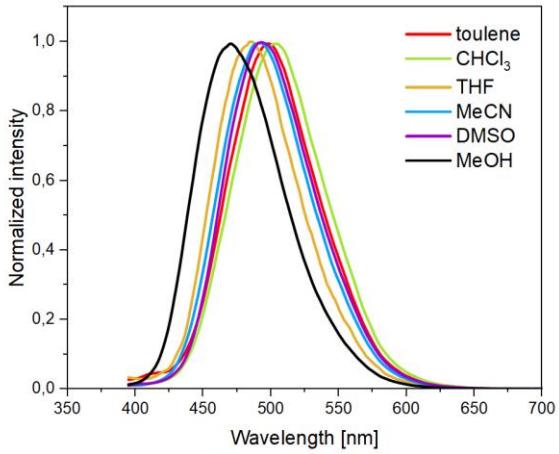

0E – absorption

c = 1 × 10^{-5} mol/L

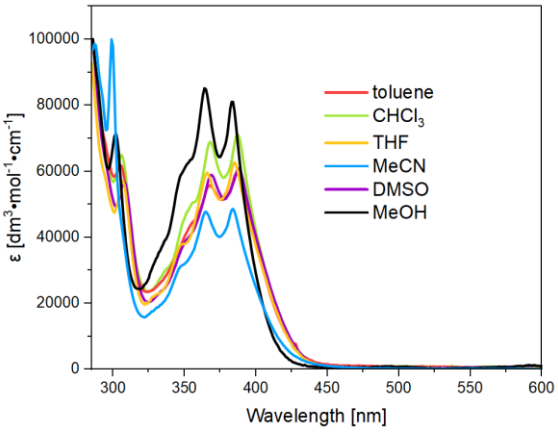

0E – aggregation

c = 1 × 10^{-5} mol/L; $\lambda_{excitation}$ = 380 nm

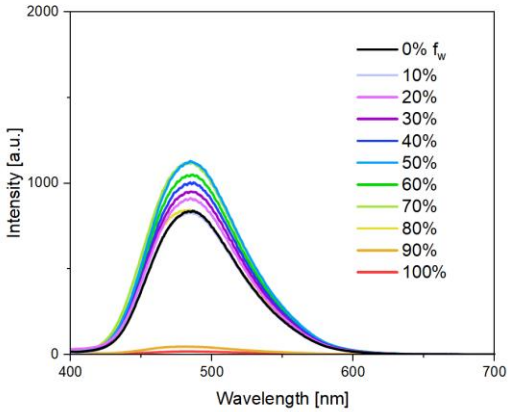

0F – absorption normalized

c = 1 × 10^{-5} mol/L

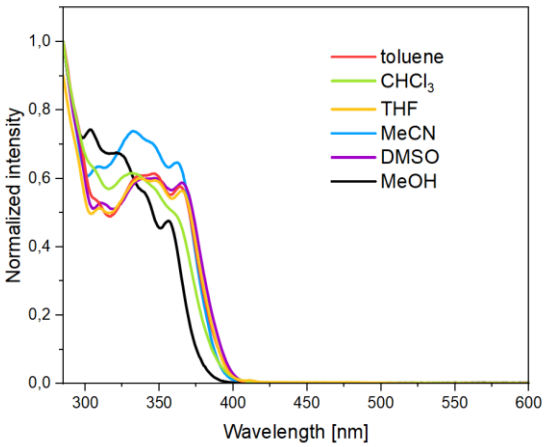

0F – emission

c = 1 × 10^{-5} mol/L; $\lambda_{excitation}$ = 380 nm

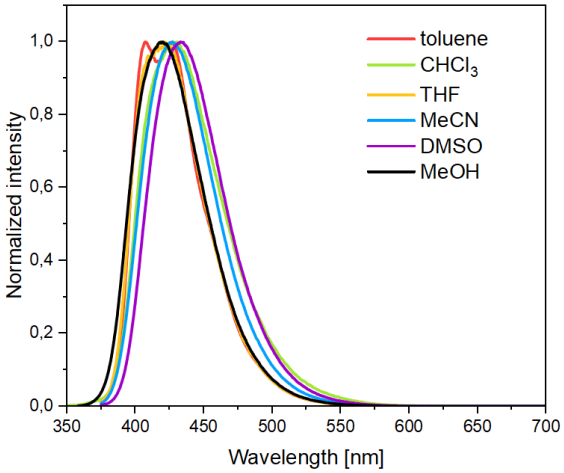

0F – absorption

c = 1 × 10^{-5} mol/L

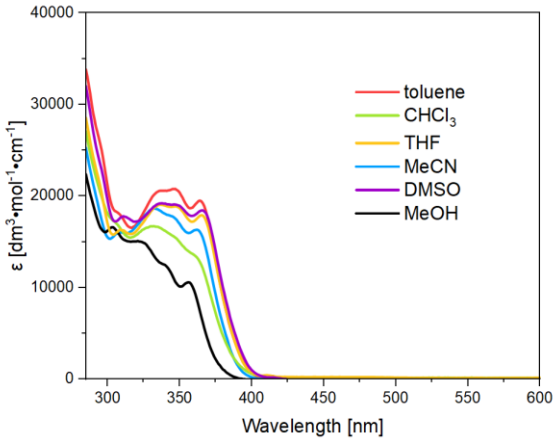

0F – aggregation

c = 1 × 10^{-5} mol/L; $\lambda_{excitation}$ = 380 nm

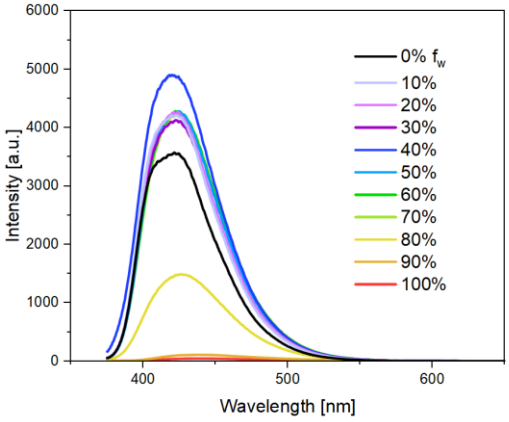

0G – absorption normalized

c = 1 × 10^{-5} mol/L

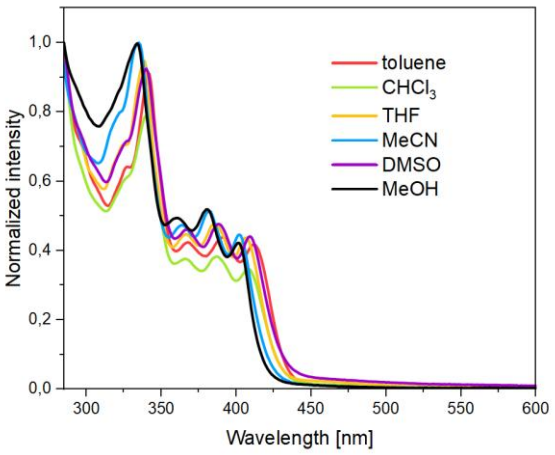

0G – emission

c = 1 × 10^{-5} mol/L; $\lambda_{excitation}$ = 395 nm

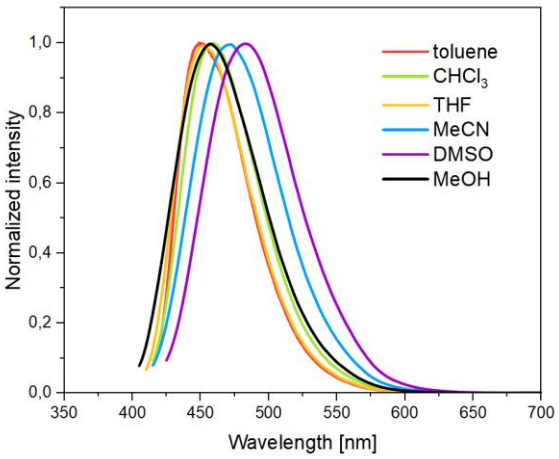

0G – absorption

c = 1 × 10^{-5} mol/L

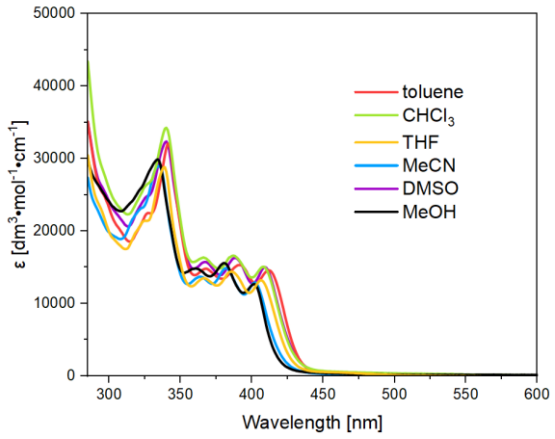

0G – aggregation

c = 1 × 10^{-5} mol/L; $\lambda_{excitation}$ = 395 nm

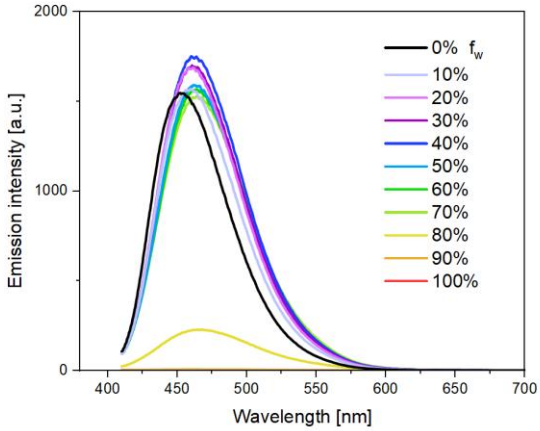

0H – absorption normalized

c = 1 × 10^{-5} mol/L

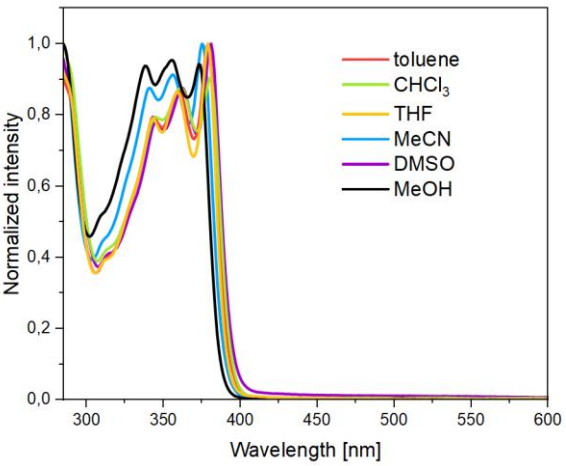

0H – emission

c = 1 × 10^{-5} mol/L; $\lambda_{excitation}$ = 360 nm

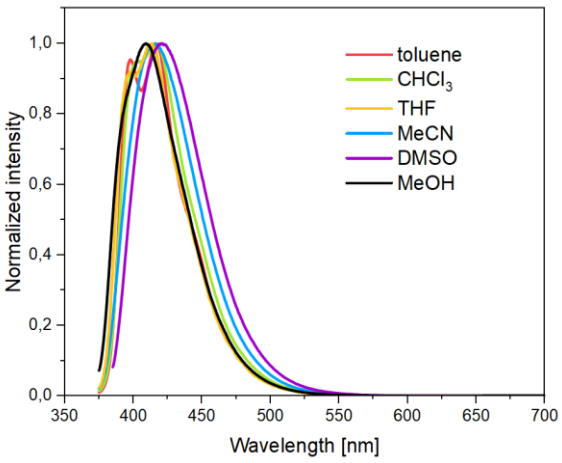

0H – absorption

c = 1 × 10^{-5} mol/L

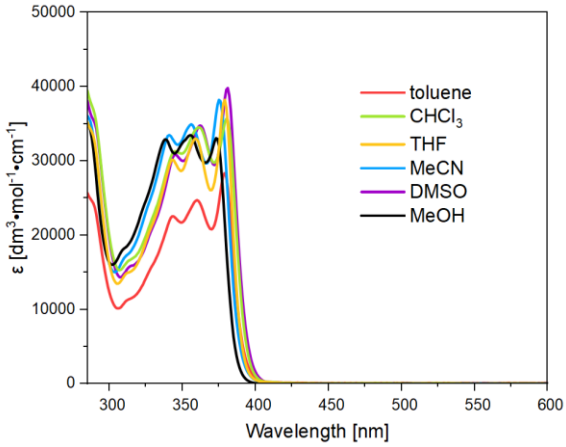

0H – aggregation

c = 1 × 10^{-5} mol/L; $\lambda_{excitation}$ = 360 nm

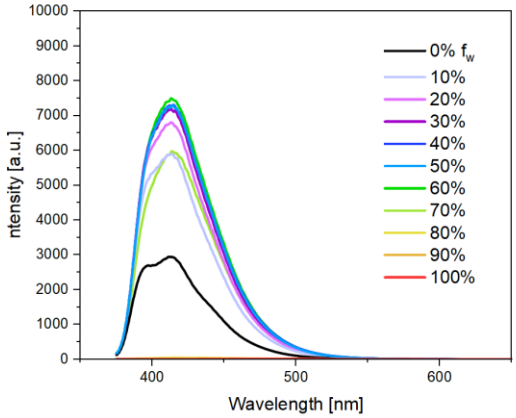

0I – absorption normalized

c = 1 × 10^{-5} mol/L

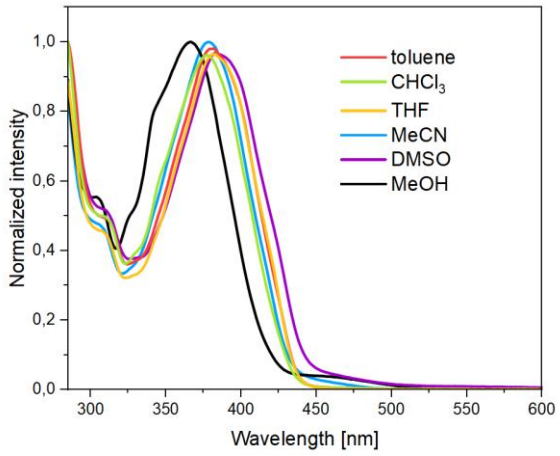

0I – emission

c = 1 × 10^{-5} mol/L; $\lambda_{excitation}$ = 380 nm

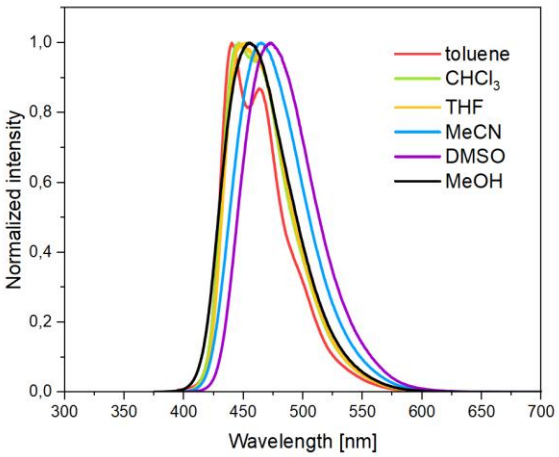

0I – absorption

c = 1 × 10^{-5} mol/L

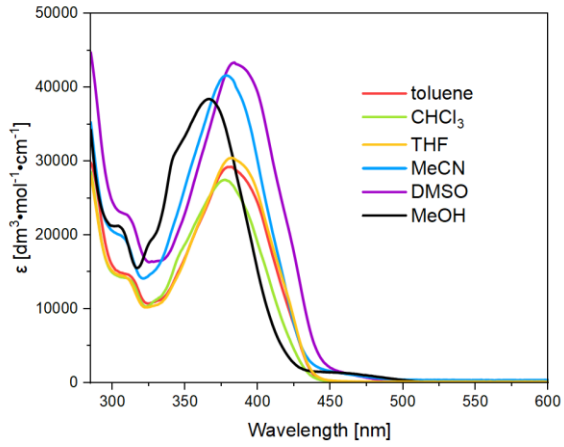

0I – aggregation

c = 1 × 10^{-5} mol/L; $\lambda_{excitation}$ = 380 nm

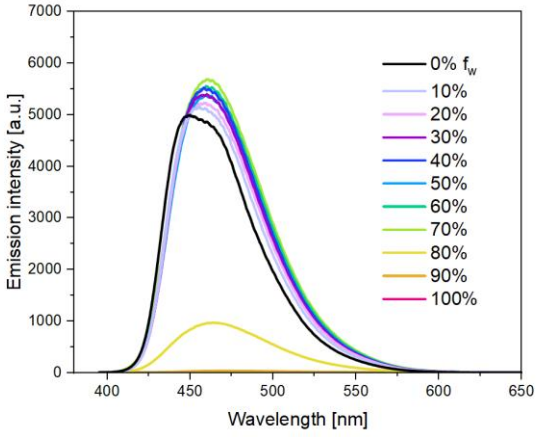

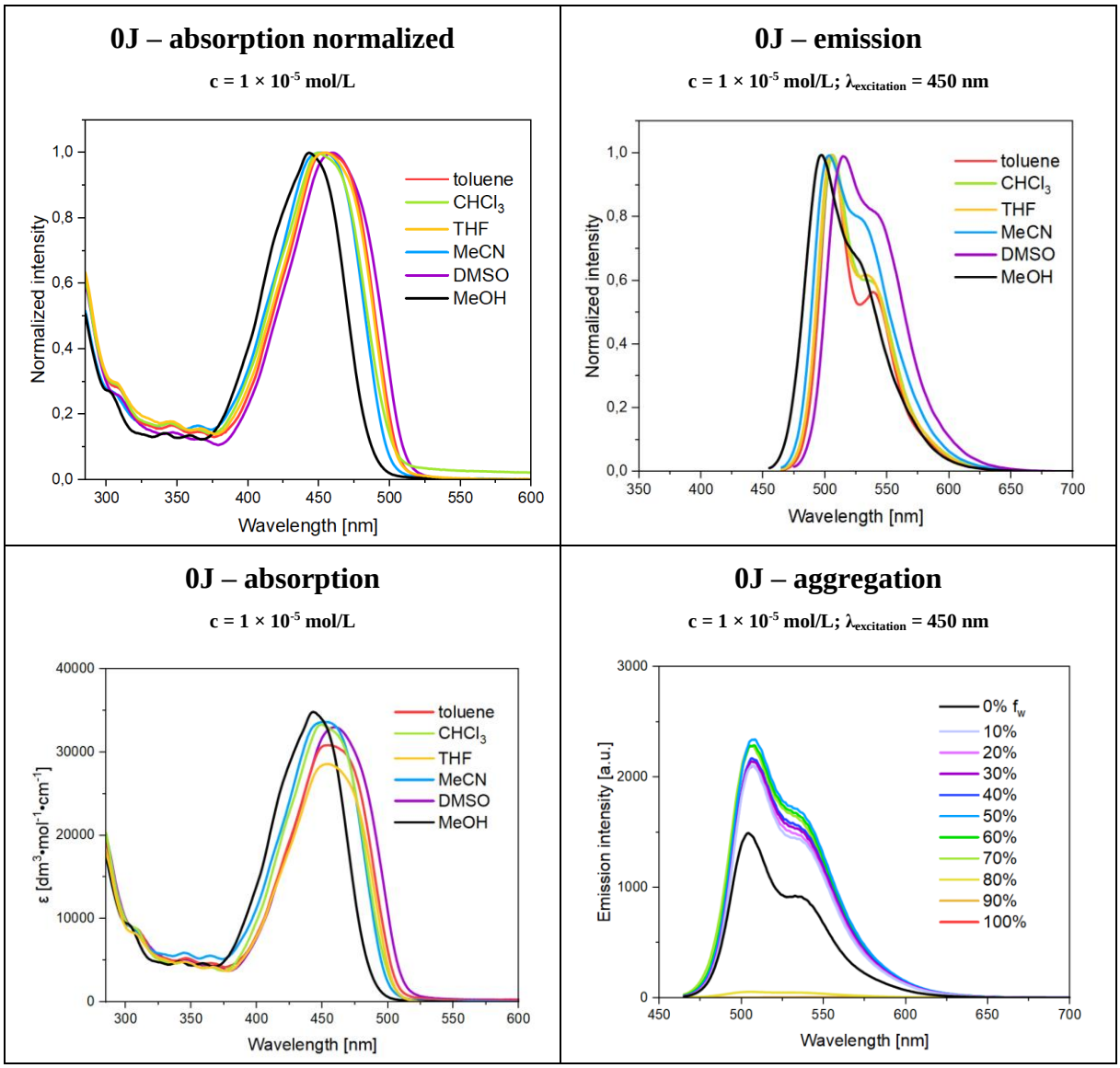

Figure S13. Absorption, emission and aggregation spectra of **0A**–**0J**.

Toluene – absorption

c = 1 × 10^{-5} mol/L

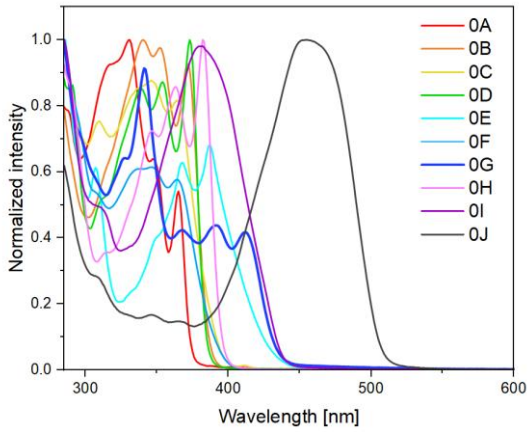

Toluene – emission

c = 1 × 10^{-5} mol/L

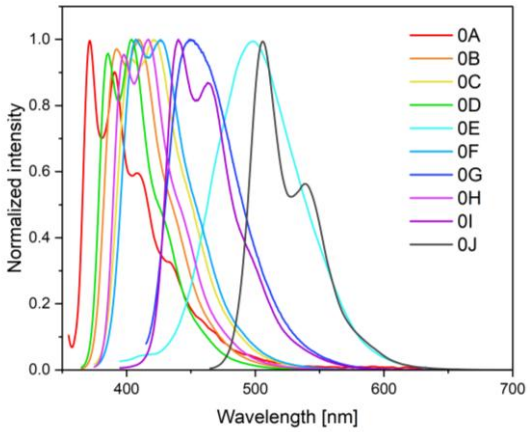

$CHCl_3$ – absorption

c = 1 × 10^{-5} mol/L

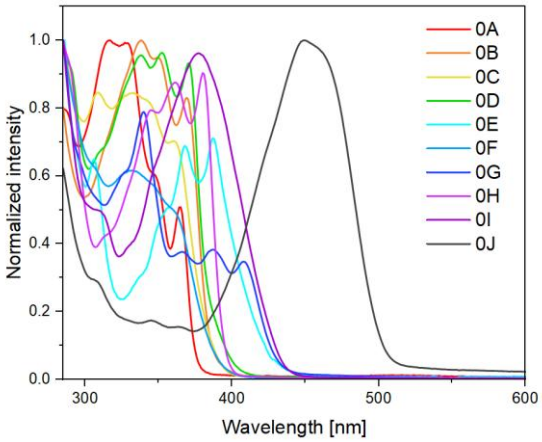

$CHCl_3$ – emission

c = 1 × 10^{-5} mol/L

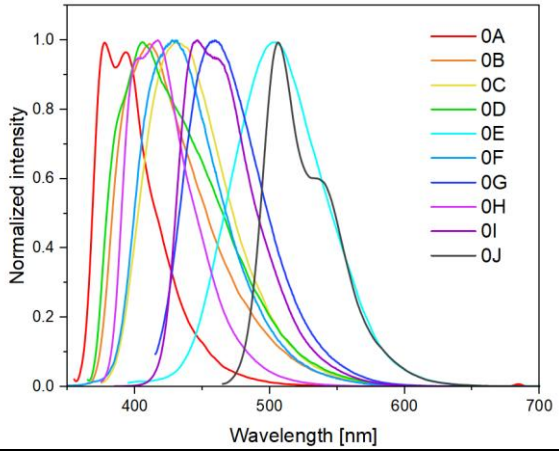

THF – absorption

c = 1 × 10^{-5} mol/L

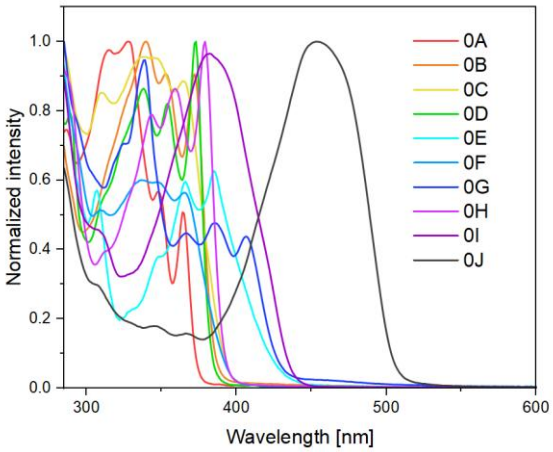

THF – emission

c = 1 × 10^{-5} mol/L

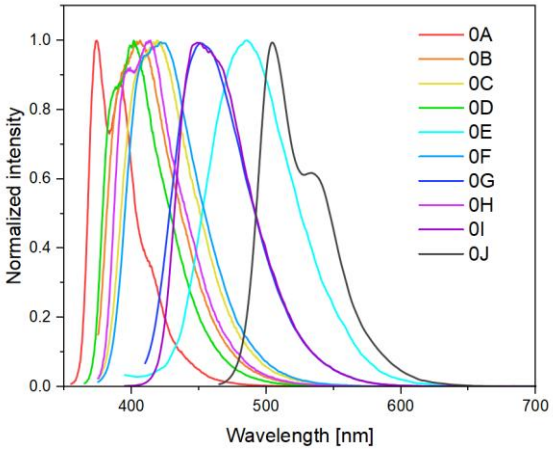

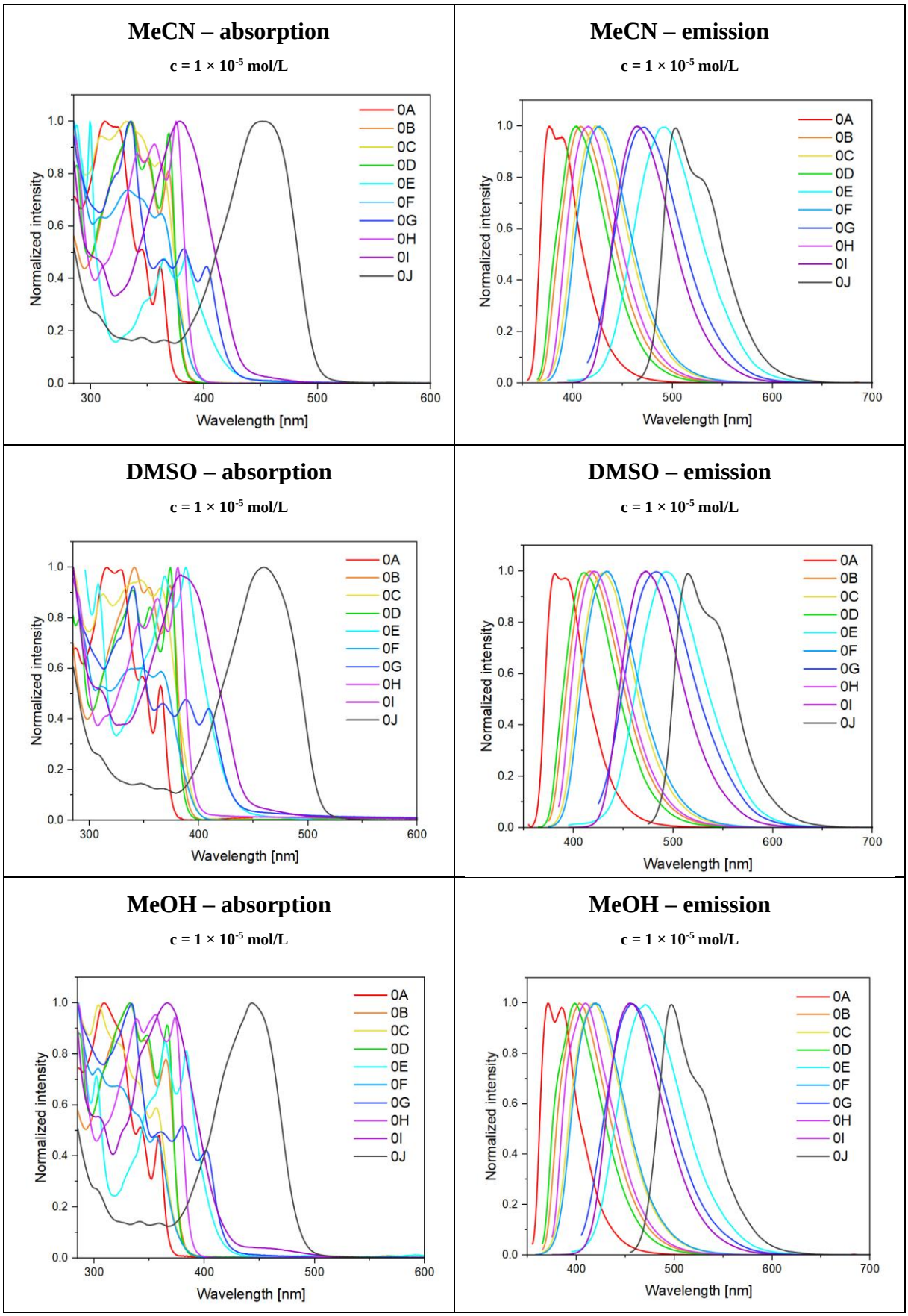

Figure S14. Comparison of absorption and emission behavior of **0A**–**0J** in solvents of varying polarity.

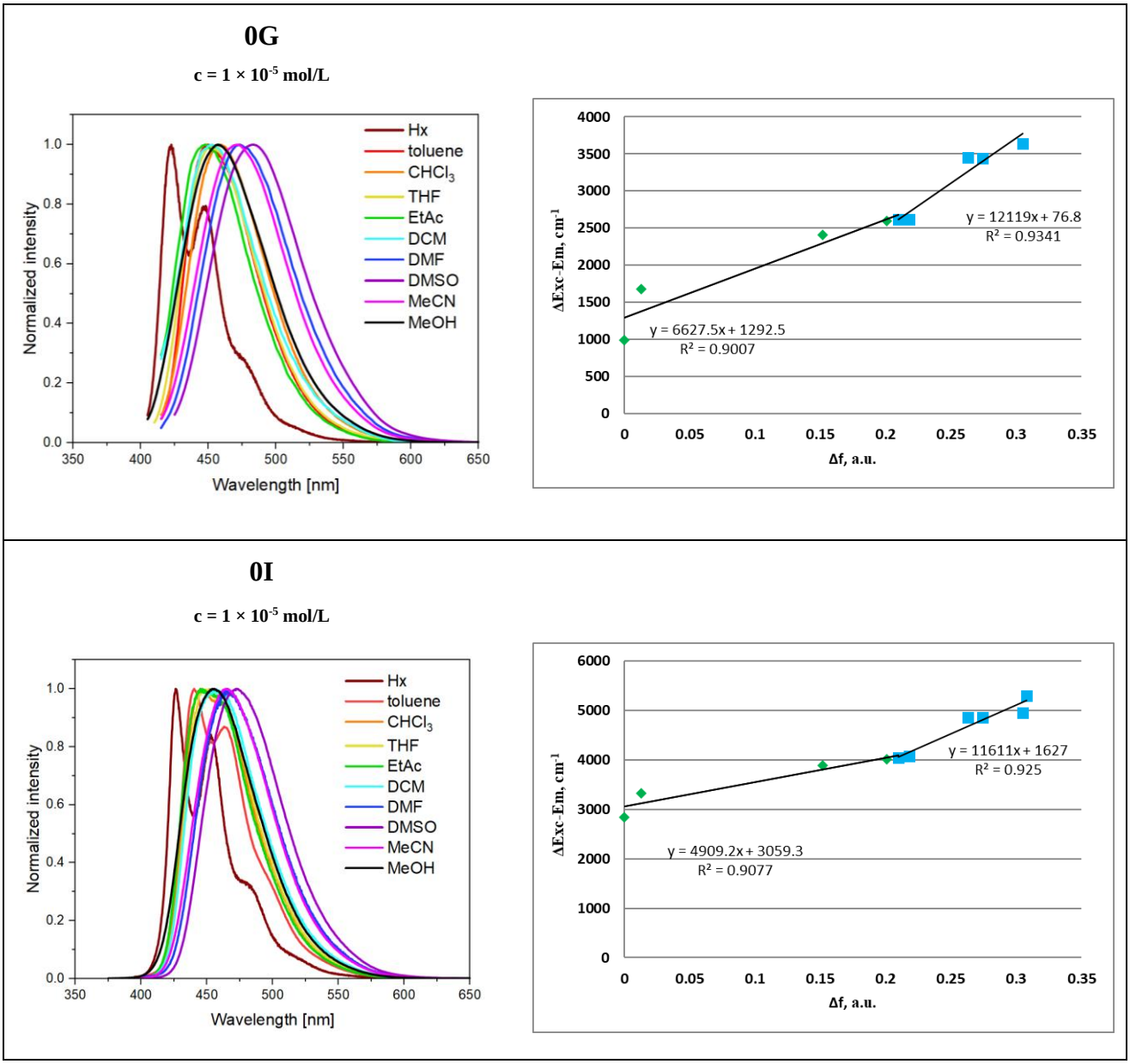

Figure S15. Lippert-Mattaga plots.

Table S2. Slope data and dipole moment values in low and high solubility solvents.

Compoud	0G	0I
slope of the line on the Lippert-Mataga plot in low polarity solvents	6627	4909
slope of the line on the Lippert-Mataga plot in high polarity solvents	12119	11611
Δμ in low polarity solvents	11.5 D	9.9 D
Δμ in high polarity solvents	15.5 D	15.2 D

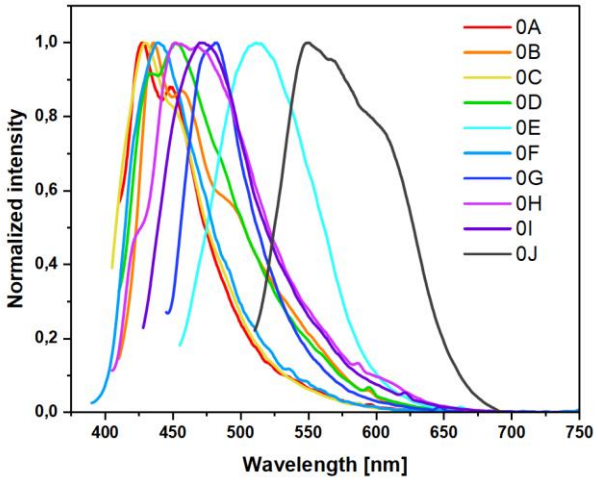

Figure S16. Solid-state spectra of **0A**–**0J**.

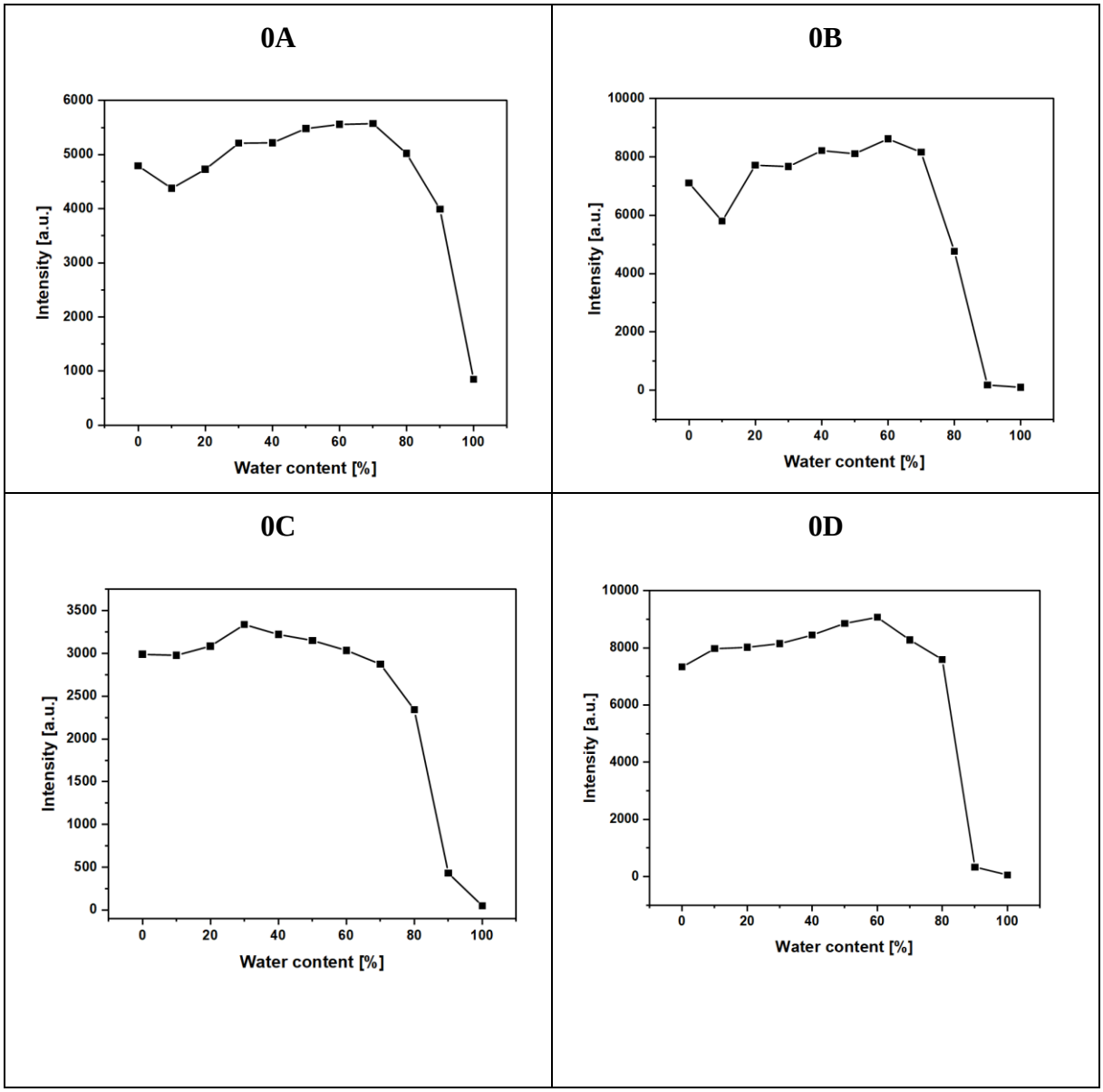

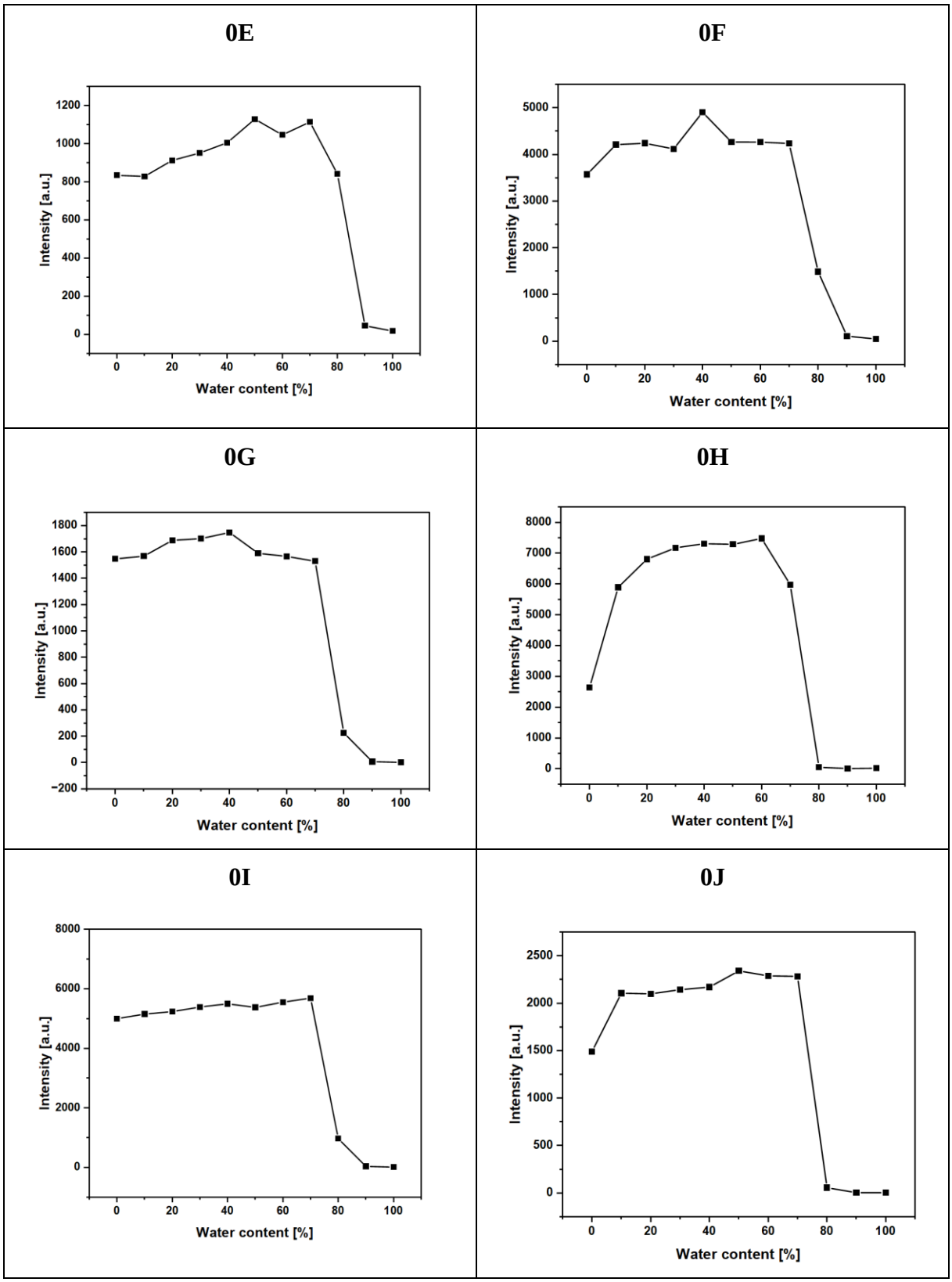

Figure S17. Change in the emission intensity of solutions in the aggregated state.

9. Photoluminescence and electroluminescent properties

Steady-state photoluminescence spectra were performed on a Edinburgh Instruments FLS980, with solvent studies performed in clean 1 cm path-length photoluminescence cuvettes (Aeika Cells). Films containing emitters in the Zeonex® matrix were prepared using toluene solvents, where the compounds and Zeonex® were initially dissolved. Subsequently, the solutions were mixed to obtain a specific concentration of the compound in the Zeonex® matrix (e.g., 1%), then then spin-coated at 2000 RPM onto sapphire substrates to form uniform layers. Samples in the CBP matrix were prepared in a chloroform solution and spin-coated at 3000 RPM onto sapphire substrates to form uniform layers.

Devices: The solution-processed OLEDs were fabricated using the spin-coating method with a 10% (*w/w*) concentration of the emitters in the CBP host. The device configuration was as follows: ITO/ PEDOT:PSS [poly(3,4-ethylenedioxythiophene):poly(styrenesulfonate) Clevios Al4083] (40 nm)/ PVKH [poly(*N*-vinylcarbazole), 1 100 000 M_w] (10 nm)/ emitter + CBP (30 nm)/ TmPyPB [1,3,5-Tris(3-pyridyl-3-phenyl)benzene] (40 nm)/LiF (1 nm)/Al (100 nm), with the last three layers deposited by evaporation. PEDOT:PSS was spin-coated after filtering at 3000 RPM for 45 s, resulting in 40 nm layers, and then annealed at 120 °C for 15 minutes. Emitters were spin-coated from a chloroform solution at 3000 RPM for 45 s without annealing. Organic semiconductors and aluminium were deposited at a rate of 1 $Å s^{-1}$, and the LiF layer was deposited at 0.1 $Å s^{-1}$. All materials were purchased from Heraeus (PEDOT:PSS) Sigma Aldrich or Lumtec and small molecules were purified by temperature-gradient sublimation in a vacuum. OLEDs have been fabricated on pre-cleaned, patterned indium-tin-oxide (ITO) coated glass substrates with a sheet resistance of 20 Ω/sq and ITO thickness of 100 nm. The sizes of pixels were 4 mm^2, 8 mm^2 and 16 mm^2. The characteristics of the devices were recorded using a 3,3-inch integrating sphere (Labsphere) inside the glovebox connected to a Source Meter Unit Keithley 2400 and Avantes Avaspec-ULS2048CL spectrometer.

10. Comparison of the results from this study with data reported in the literature

Table S3. Comparison of selected physicochemical properties of **0A**–**0J** derivatives and OLED parameters with literature data.

Compound	T_m/T_5 (°C)	HOMO/LUMO (eV)	Eg_{opt} (eV)	$PLQY_{sol/film}$ (%)	λ_{EL} (nm)	L_{max} (cd/m^2)	EQE_{max} (%)	CIE (x,y)	Ref.
0A	-/292	-5.86/-1.45	3.31	DMSO 0.33 (QY_{AE}) $CHCl_3$ 15/18 (CBP)	402 (CBP film)	6963	2.67	0.1925, 0.1633	This work
0B	270/337	-5.80/-1.67	3.22	DMSO 0.47 (QY_{AE}) $CHCl_3$ 30/13 (CBP)	420 (CBP film)	3578	1.03	0.1819, 0.1311	This work
0C	228/308	-5.85/-1.68	3.16	DMSO 0.29 (QY_{AE}) $CHCl_3$ 17/18 (CBP)	430 (CBP film)	1963	1.20	0.1645, 0.0849	This work
0D	248/314	-5.82/-1.74	3.20	DMSO 0.35 (QY_{AE}) $CHCl_3$ 24/5 (CBP)	421 (CBP film)	3000	0.37	0.2035, 0.2037	This work
0E	-/327	-5.80/-2.14	2.94	DMSO 0.29 (QY_{AE}) $CHCl_3$ 23/13 (CBP)	477 (CBP film)	4221	2.62	0.1828, 0.2634	This work
0F	-/313	-5.86/-1.72	3.20	DMSO 0.34 (QY_{AE}) $CHCl_3$ 20/18 (CBP)	435 (CBP film)	5192	1.23	0.1670, 0.1017	This work
0G	271/313	-5.68/-2.17	2.87	DMSO 0.30 (QY_{AE}) $CHCl_3$ 39/15 (CBP)	459 (CBP film)	3620	1.11	0.1714, 0.1417	This work
0H	298/363	-5.80/-1.78	3.16	DMSO 0.46 (QY_{AE}) $CHCl_3$ 35/12 (CBP)	432 (CBP film)	3277	0.92	0.2002, 0.2176	This work
0I	318/362	-5.68/-2.06	2.88	DMSO 0.34 (QY_{AE}) $CHCl_3$ 35/11 (CBP)	475 (CBP film)	4190	2.12	0.1794, 0.2668	This work
0J	321/317	-5.49/-2.42	2.46	DMSO 0.36 (QY_{AE}) $CHCl_3$ 35/23 (CBP)	566 (CBP film)	8962	4.29	0.3802, 0.5643	This work
ACPI	290/410	-5.62/-2.54	-	0.87/-	456	11470	3.52	0.156, 0.155	[3]
1-NaCPI	345/441	-5.58/-2.56	-	0.71/-	468	16000	2.88	0.165, 0.199	[3]
2-NaCPI	354/473	-5.55/-2.55	-	0.62/-	460	12250	3.61	0.150, 0.160	[3]
ANPI	288/396	-5.76/-2.66	-	0.62/-	472	7554	1.56	0.166, 0.213	[4]
2-NaNPI	365/469	-5.75/-2.64	-	0.61/-	460	9224	2.71	0.154, 0.147	[4]
PNPI	230/446	-5.77/-2.45	-	0.48/-	462	12250	2.82	0.153, 0.163	[4]

p-PABPI	-/511	-5.59/-2.65	2.94	-/0.74	444	9539	3.92	0.15,0.09	[5]
m-PABPI	-/438	-5.37/-2.39	2.98	-/0.56	436	4091	2.24	0.15,0.04	[5]
PIMNA	297/371	-5.62/-2.21	3.37	79/82	412	6580	2.21	0.160, 0.034	[6]
1	-/363	-6.20/-3.11	3.09	0.40/-	460	5168	0.83	0.16, 0.17	[7]
2	-/400	-6.08/-3.02	3.06	0.76/-	448	5118	0.85	0.15, 0.12	[7]
1	296/371	-5.62/-2.21	3.37	77/82	412	6580	2.43	0.160, 0.035	[8]
2	-/421	-5.52/-2.52	3.01	90/57	448	54300	5.11	0.154, 0.141	[8]
3	326/386	-5.62/-2.64	2.98	41/34	460	35600	2.29	0.164, 0.185	[8]
BBAB	205/280	-5.67/-2.54	3.10	-/0.42 (solid)	448	-	1.53	0.15, 0.12	[9]
2N-PI	220/363	-5.33/-2.27	3.06	-/0.70 (solid)	448	-	0.95	0.15, 0.11	[9]
Anthracene-PI	325/337	-5.51/-2.43	3.08	-/0.82 (solid)	472	-	0.80	0.16, 0.24	[9]
Ph-BPI	244/351	-5.41/-2.39	3.02	-/0.65 (solid)	448	-	0.68	0.15, 0.10	[9]
1N-BPI	230/378	-5.41/-2.38	3.03	-/0.74 (solid)	448	-	0.60	0.14, 0.10	[9]
2N-BPI	196/386	-5.27/-2.37	2.90	-/0.88 (solid)	448	-	1.61	0.14, 0.11	[9]
2N-API	279/390	-5.59/-2.37	3.13	-/0.58 (solid)	448	-	1.47	0.15, 0.11	[9]
Py-BPI	300/429	-5.35/-2.68	2.67	-/0.80 (solid)	468	-	2.0	0.15, 0.19	[9]
TPI	-/307	-5.62/-2.35	3.27	-/0.15	420	-	0.96	0.163, 0.076	[10]
TPI-Bz	-/423	-5.52/-2.40	3.12	-/0.43	420	-	1.45	0.162, 0.043	[10]
TPI-2Na	-/502	-5.49/-2.43	3.06	-/0.61	428	-	1.98	0.161, 0.063	[10]
TPI-1Na	-/456	-5.55/-2.39	3.16	-/0.31	420	-	0.83	0.184, 0.116	[10]
TPI-Ph	-/483	-5.54/-2.38	3.16	-/0.72	428	-	3.72	0.158, 0.050	[10]
TPI-An	-/479	-5.53/-2.56	2.97	-/0.69	448	-	3.39	0.200, 0.221	[10]
TPI-Py	-/542	-5.50/-2.54	2.96	-/0.93	460	-	5.69	0.157, 0.177	[10]
1	210/351	-5.62/-2.64	3.16	60/62	404	36 823	2.13	0.16,0.13	[11]
2	212/362	-5.30/-2.26	3.04	63/68	417	38 032	2.26	0.15, 0.12	[11]
3	220/401	-5.29/-2.49	2.80	68/49	450	53 890	5.30	0.15,0.14	[11]

11. Literature

[1] D. Gobel, N. Clamor, E. Lork, B. J. Nachtsheim, Org. Lett. 2019, 21, 5373−5377

[2] F. J. Steemers, W. Verboom, D. N. Reinhoudt, E. B. van der Tol, J. W. Verhoeven, J. Am. Chem. Soc., 1995,117, 9408-9414.

[3] S. Zhuang, R. Shangguan, J. Jin, G. Tu, L. Wang, J. Chen, D. Ma and X. Zhu, Org. Electron., 2012, 13, 3050–3059.

[4] S. Zhuang, R. Shangguan, H. Huang, G. Tu, L. Wang and X. Zhu, Dyes Pigm., 2014, 101, 93–102.

[5] J. Wang, X. Lou, Y. Liu, G. Zhao, A. Islam, S. Wang and Z. Ge, Dyes Pigm., 2015, 118, 137–144.

[6] T. Shan, Y. Liu, X. Tang, Q. Bai, Y. Gao, Z. Gao, J. Li, J. Deng, B. Yang, P. Lu and Y. Ma, ACS Appl. Mater. Interfaces, 2016, 8, 28771–28779.

[7] F. Zhang, W. Li, D. Wei, X. Wei, Z. Li, S. Zhang, S. Li, B. Wei, G. Cao and B. Zhai, RSC Adv., 2016, 6, 60264–60270.
[8] T. Shan, Z. Gao, X. Tang, X. He, Y. Gao, J. Li, X. Sun, Y. Liu, H. Liu, B. Yang, P. Lu and Y. Ma, Dyes Pigm., 2017, 142, 189–197.
[9] Y. Zhang, J.-H. Wang, G. Han, F. Lu and Q.-X. Tong, RSC Adv., 2016, 6, 70800–70809.
[10] W.-C. Chen, Y. Yuan, Y. Xiong, A. L. Rogach, Q.-X. Tong and C.-S. Lee, ACS Appl. Mater. Interfaces, 2017, 9, 26268–26278.
[11] J. Jayabharathi, R. Ramya, V. Thanikachalam and P. Nethaji, RSC Adv., 2018, 8, 29031–29043.